Atmos. Chem. Phys., 22, 8701–8723, 2022
https://doi.org/10.5194/acp-22-8701-2022

Atmospheric Chemistry and Physics
Open Access
EGU

Nine-year trends of PM_{10} sources and oxidative potential in a rural background site in France

Lucille Joanna Borlaza[1], Samuël Weber[1], Anouk Marsal[1], Gaëlle Uzu[1], Véronique Jacob[1], Jean-Luc Besombes[2], Mélodie Chatain[3], Sébastien Conil[4], and Jean-Luc Jaffrezo[1]

[1]University of Grenoble Alps, CNRS, IRD, INP-G, IGE (UMR 5001), 38000 Grenoble, France
[2]Université Savoie Mont-Blanc, CNRS, EDYTEM (UMR5204), 73000 Chambéry, France
[3]Atmo Grand Est, 67300 Schiltigheim, France
[4]ANDRA, DRD/GES Observatoire Pérenne de l'Environnement, 55290 Bure, France

Correspondence: Lucille Joanna Borlaza (lucille-joanna.borlaza@univ-grenoble-alpes.fr) and Jean-Luc Jaffrezo (jaffrezo@univ-grenoble-alpes.fr)

Received: 8 October 2021 – Discussion started: 29 November 2021
Revised: 17 June 2022 – Accepted: 21 June 2022 – Published: 6 July 2022

Abstract. Long-term monitoring at sites with relatively low particulate pollution could provide an opportunity to identify changes in pollutant concentration and potential effects of current air quality policies. In this study, 9-year sampling of PM_{10} (particles with an aerodynamic diameter below 10 µm) was performed in a rural background site in France (Observatoire Pérenne de l'Environnement or OPE) from 28 February 2012 to 22 December 2020. The positive matrix factorization (PMF) method was used to apportion sources of PM_{10} based on quantified chemical constituents and specific chemical tracers analysed on collected filters. Oxidative potential (OP), an emerging health metric that measures PM capability to potentially cause anti-oxidant imbalance in the lung, was also measured using two acellular assays: dithiothreitol (DTT) and ascorbic acid (AA). The sources of OP were also estimated using multiple linear regression (MLR) analysis. In terms of mass contribution, the dominant sources are secondary aerosols (nitrate- and sulfate-rich) associated with long-range transport (LRT). However, in terms of OP contributions, the main drivers are traffic, mineral dust, and biomass burning factors. There is also some OP contribution apportioned to the sulfate- and nitrate-rich sources influenced by processes and ageing during LRT that could have encouraged mixing with other anthropogenic sources. The study indicates much lower OP values than in urban areas. A substantial decrease (58 % reduction from the year 2012 to 2020) in the mass contributions from the traffic factor was found, even though this is not clearly reflected in its OP contribution. Nevertheless, the findings in this long-term study at the OPE site could indicate effectiveness of implemented emission control policies, as also seen in other long-term studies conducted in Europe, mainly for urban areas.

1 Introduction

Particulate matter (PM) pollution causes various environmental concerns affecting public health and climate. An overwhelming part of the scientific literature on PM chemical characterization and sources focuses on urban and populated areas, where most emissions originate from and where populations are impacted. Further work has also been carried out in more specific areas to understand particular processes of aerosol formation and transport, as well as specific sources such as in the boreal forest (Yan et al., 2016), polar environments (Barrie and Hoff, 1985; Moroni et al., 2016), high altitude (Rinaldi et al., 2015), or marine sites (Scerri et al., 2016). Rural sites are of great interest as well because they can represent the regional background of the atmosphere and potential influence from long-range transport (LRT) of pollutants. Studies at such sites provide more understanding of large-scale and mesoscale processes (Anenberg et al., 2010; Mues et al., 2013; Konovalov et al., 2009), which can be useful in chemical transport models. The continuation of these

studies could lead to the identification of long-term trends and the effect of recent changes in the source emissions. Indeed, several programmes have been set to monitor atmospheric composition in a harmonized way for background areas throughout Europe and North America. Among these are ACTRIS (Aerosol, Clouds and Trace Gases Research Infrastructure) (Pappalardo, 2018), EMEP (European Monitoring and Evaluation Programme) (Aas et al., 2012; Alastuey et al., 2016), IMPROVE (Interagency Monitoring of Protected Visual Environments) (Hand et al., 2012), and CAPMoN (Canadian Air and Precipitation Monitoring Network) (Nejedlý et al., 1998). However, only few sites provide long-term in-depth series of PM chemical speciation data.

Further, although current air quality standards are based on ambient mass concentration of PM, there is also a growing interest in new types of characterization that take into account not only particle composition, but also its capability to generate health impacts (Park et al., 2018; Crobeddu et al., 2017; Møller et al., 2010; Bates et al., 2019). This is the case of PM oxidative potential (OP) (Nel, 2005; Conte et al., 2017; Yang et al., 2014; Verma et al., 2014), the ability of PM to generate reactive oxygen species (ROS) leading to PM-induced oxidative stress in the lungs. In France, several studies have reported about the OP of ambient PM in different urban environments (Weber et al., 2018, 2021; Borlaza et al., 2021b; Calas et al., 2019; Daellenbach et al., 2020), but there are still limited studies performed in rural areas. The characterization of PM sources and OP in a rural site will enable us to investigate the large-scale effects of mitigation policies that target reduction of PM mass concentrations. This will also provide knowledge of the efficiency of current air quality guidelines in terms of other emerging health-based metrics of PM exposure.

The understanding of trends of PM is essential to evaluate the effects of mitigation policies on air pollution levels. A reference background site offers a good opportunity to gauge the broad effects of certain improvements in the transportation fleet and other regulations aimed at reducing vehicular emissions in large cities. Thus, in this study, an extensive dataset of PM over a 9-year period ($n = 434$), obtained from a French national background site, was investigated to (1) provide insights on the long-term trends of PM sources and other emerging health-based metrics of PM exposure, such as OP of PM, and (2) quantify the temporal evolution of the contributions of these sources, particularly focusing on vehicular emissions that have already been shown to decrease in urban environments in Europe during the last decades.

2 Methodology

2.1 Site description and sampling parameters

The OPE (Observatoire Pérenne de l'Environnement) sampling site is managed by the French national radioactive waste management agency (ANDRA). It is located in a remote area in the north-eastern part of France (48.5° N, 5.5° E) at an altitude of 390 m above sea level, in a large agricultural area without any residential areas within several kilometres (Fig. 1). The mean annual temperature between 2011 and 2018 in the area was 10.5 °C [minimum, maximum: −15.2 °C, 36.4 °C], average cumulated yearly precipitation was 829 mm, and the predominant local wind regimes are south-westerly and east-north-easterly winds (Conil et al., 2019). This site, being far from any local anthropogenic sources, is considered representative of the rural atmospheric background of north-eastern France. Golly et al. (2019) also demonstrated that the PM chemistry at this site is very close to that in several other background rural sites in France.

The PM_{10} samples in this study were collected from 28 February 2012 to 22 December 2020. Particularly, from 28 February 2012 to 28 December 2015, the samples ($n = 181$) were collected on a weekly basis (from Tuesday 09:00 CET to Tuesday 09:00 CET) using a low volume sampler (Partisol, 1 $m^3\,h^{-1}$) onto 47 mm diameter quartz fibre filters (Tissuquartz PALL QAT-UP 2500 diameter 47 mm). From 12 January 2016 to 22 December 2020, the samples ($n = 253$) were collected on a daily (24 h) basis in a 6 d sampling interval using a high-volume sampler (Digitel DA80, 30 $m^3\,h^{-1}$) onto 150 mm diameter quartz fibre filters (Tissuquartz PALL QAT-UP 2500 diameter 150 mm).

All filters were preheated at 500 °C for 12 h before use to avoid organic contamination. Blank filters (about 10 % by number of the actual filters) were also collected to quantify detection limits and to secure the absence of contamination during sample transport, setup, and recovery. After collection, all filter samples were wrapped in aluminium foil, sealed in zipper plastic bags, and stored at < 4 °C until further chemical analysis.

2.2 Chemical analyses

After collection, samples were subject to various chemical analyses to perform the quantification of the major constituents by mass and specific chemical tracers of sources needed for the positive matrix factorization (PMF) model. These analyses were performed in the same laboratory for all samples ($n = 434$) during the entire sampling duration (28 February 2012 to 22 December 2020).

The carbonaceous components (organic carbon (OC) and elemental carbon (EC)) were analysed using a thermo-optical method on a Sunset Lab analyser (Birch and Cary, 1996), using the EUSAAR2 temperature programme. Total organic matter (OM) in daily ambient PM_{10} was estimated by multiplying the OC mass concentration by a factor of 1.8. Yazdani et al. (2021) showed that this is consistent with the range estimated for rural samples from the IMPROVE network that is generally higher than for urban samples.

A set of other chemical analyses was performed on a single water extraction of each filter. This extraction was performed in 10 mL of ultra-pure water under vortex agitation

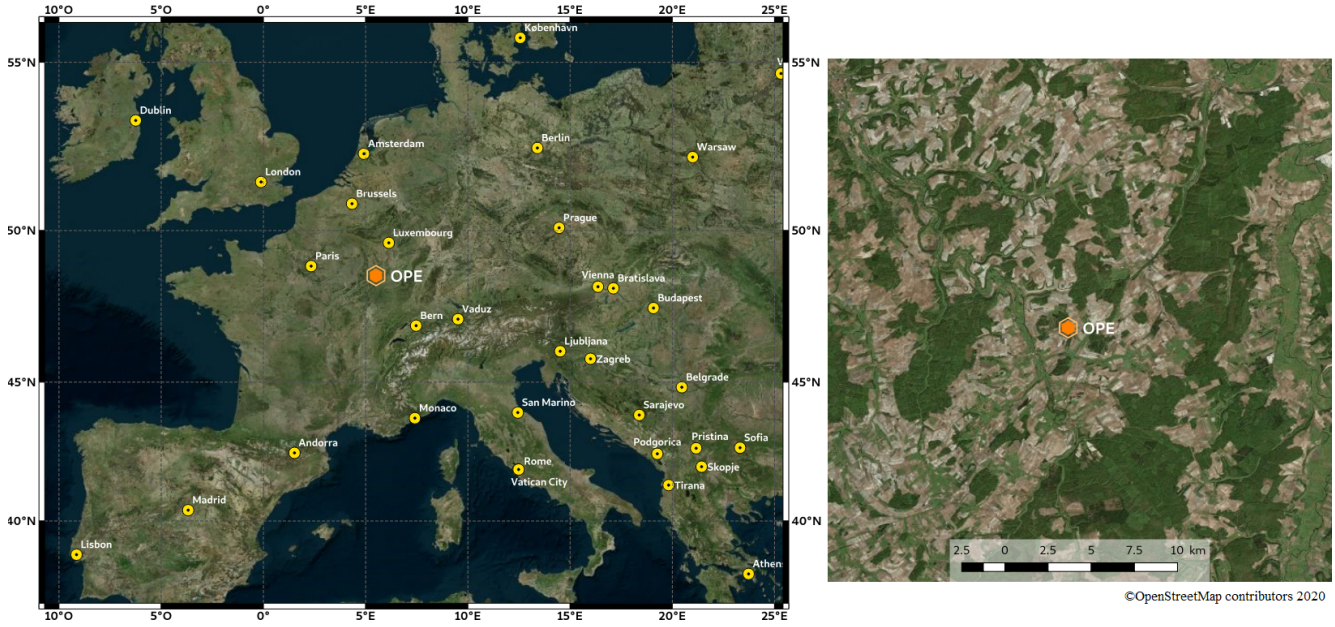

Figure 1. Location of the OPE site in France. © OpenStreetMap contributors 2020. Distributed under a Creative Commons BY-SA License.

for 20 min. The extract was then filtered with a 0.22 µm porosity Nuclepore filter. The major ionic components (Na^+, NH_4^+, K^+, Mg^{2+}, Ca^{2+}, Cl^-, NO_3^-, SO_4^{2-}) and methane sulfonic acid (MSA) were measured by ion chromatography (IC, Thermo Fisher ICS 3000) following a standard protocol described in Jaffrezo et al. (1998) and Waked et al. (2014). An ICS300 (Thermo-Fisher) with AS11 HC column for the anions and CS16 for the cations was used.

The analyses of anhydro-sugars and primary saccharides were achieved using high-performance liquid chromatography with pulsed amperometric detection (HPLC-PAD). The samples collected before the year 2017 were analysed using a set of Metrohm columns (Metrosep A Supp 15 and Metrosep Carb1) on Dionex DX500 HPLC. The samples collected after the year 2017 were analysed with a Thermo-Fisher ICS 5000+ HPLC equipped with 4 mm diameter Metrosep Carb 2 × 150 mm column and 50 mm pre-column. The analytical run is isocratic, with 15 % of an eluent of sodium hydroxide (200 mM) and sodium acetate (4 mM) and 85 % water, at 1 mL min^{-1}. These methods allowed for the quantification of anhydrous saccharides (levoglucosan and mannosan) and polyols (sum of arabitol and mannitol), as described in detail in Waked et al. (2014) and Samaké et al. (2019).

Trace elements were analysed after mineralization, using 5 mL of HNO_3 (70 %) and 1.25 mL of H_2O_2 during 30 min at 180 °C in a microwave oven (microwave MARS 6, CEM). The elemental analysis (Al, As, Ba, Ca, Cd, Ce, Co, Cr, Cs, Cu, Fe, K, La, Li, Mg, Mn, Mo, Ni, Pb, Pd, Pt, Rb, Sb, Se, Sn, Sr, Ti, Tl, V, Zn, Zr) was performed on this extract using inductively coupled plasma mass spectroscopy (ICP-MS) (ELAN 6100 DRC II PerkinElmer or NEXION PerkinElmer), as described by Alleman et al. (2010).

All procedures have been performed following the related EN standards (i.e. EN 12341, EN 14902, EN 16909, EN 16913). A quality control of the chemical analyses, including a mass closure test, is available in the Supplement (see Sect. S1). A summary of the quantification limits (QLs) on each chemical species measured at the OPE site is also provided in Table S1. Finally, our group successfully and regularly participates in inter-laboratory comparison exercises for OC and EC within ACTRIS and in EMEP (European Monitoring and Evaluation Programme) for ion analysis. The PM_{10} measurements from the tapered element oscillating microbalance (TEOM) are all in a daily (24 h, 09:00 to 09:00 CET) resolution, while the reconstructed PM_{10} were obtained from chemical analysis performed on filters collected on a weekly (7 d, 09:00 to 09:00 CET) or daily (24 h, 09:00 to 09:00 CET) basis. A total of 299 out of 434 (69 %) TEOM measurements were paired with reconstructed PM_{10} data, due to many interruptions in the TEOM functioning, in order to evaluate the semi-volatile mass missing in the mass reconstruction with filter chemistry.

2.3 Oxidative potential (OP) analysis

The OP analysis was performed on PM_{10} extracts from collected filter samples using a simulated lung fluid (SLF) solution composed of a Gamble + DPPC (dipalmitoylphosphatidylcholine) at 25 µg mL^{-1} iso-mass concentration (Calas et al., 2017). This methodology facilitates particle extraction in conditions closer to lung physiology. The OP analysis only started on samples collected from 13 June

2017 to 22 December 2020, amounting to a total of 191 samples.

Two assays were used to characterize OP activity: (1) dithiothreitol (DTT) and (2) ascorbic acid (AA) assays, as briefly described in the following sections. The volume-normalized OP activity (OP_v) is the OP consumption (nmol min^{-1}) normalized by the sampled air volume (m^3), representing the OP exposure in each sample. All samples analysed were subjected to triplicate analysis, and each sample results in the mean of such a triplicate. The common coefficient of variation (CV) is between 0 % and 10 % for each assay.

DTT is used as a chemical surrogate to mimic in vivo interaction of PM with biological reducing agents, such as adenine dinucleotide (NADH) and nicotinamide adenine dinucleotide phosphate (NADPH), in the DTT assay. The consumption of DTT in the assay represents the ability of PM to generate ROS (i.e. superoxide radical formation) (Cho et al., 2005). The PM_{10} extract is mixed with the DTT solution. Afterwards, the remaining DTT that did not react with PM_{10} is reacted with 5,50-dithiobis-(2-nitrobenzoic acid) (DTNB). This reaction produces 5-mercapto-2-nitrobenzoic acid or TNB. The TNB is measured by absorbance at 412 nm wavelength using a plate reader (TECAN spectrophotometer Infinite M200 Pro) with 96-well plates (CELLSTAR, Greiner-Bio) in a 10 min time step interval for a total of 30 min of analysis time.

AA is a known antioxidant used in AA assays using a respiratory tract lining fluid (RTFL) (Kelly and Mudway, 2003). This antioxidant prevents the oxidation of lipids and proteins in the lung lining fluid (Valko et al., 2005). The consumption of AA also represents PM-induced depletion of a chemical proxy (i.e. cellular AA antioxidant). The mixture (PM_{10} extracts reacted with AA) is injected into a 96-well multiwall UV-transparent plate (CELLSTAR, Greiner-Bio) and measured at 265 nm absorbance using a plate reader (TECAN spectrophotometer Infinite M200 Pro) in a 4 min time step interval for a total of 30 min of analysis time.

Both DTT and AA assays measure OP by depletion of specific chemical proxies, cellular reductants (for DTT), and antioxidants (for AA). Studies have well identified a large number of PM constituents that influence OP concentrations. At least, OP assays are known to be associated with some metals (Cu, Fe, and Mn, among others) and some organic species (especially photochemically sensitive species such as quinones) (Calas et al., 2017, 2019; Charrier et al., 2014; Pietrogrande et al., 2019). However, in ambient air, each assay reports its own associations that may vary according to the local context (emission sources, local transport leading to various ageing processes and spatio-temporal variations) (Gao et al., 2020a). Hence, a synergetic approach using multiple OP assays, to capture the most complete information regarding PM reactivity, is commonly suggested (Bates et al., 2019; Calas et al., 2017; Borlaza et al., 2021b).

In every experiment, a positive control test is performed to ensure the accuracy and precision of measurements. A 1,4-naphthoquinone (1,4-NQ) solution was used for both DTT (40 µL of 24.7 µM stock solution) and AA (80 µL of 24.7 µM 1,4-NQ solution) assays. The CV of the positive controls was < 3 % for the two assays. Additionally, an ambient filter collected from the lab roof (with an expected constant OP value) was added on each microplate to ensure precision of OP measurements.

2.4 Source apportionment

2.4.1 PMF model and input variables

The United States Environmental Protection Agency Positive Matrix Factorization (EPA PMF 5.0) software (Norris et al., 2014) was used to identify and quantify the major sources of PM_{10}. PMF is a receptor model fully described by Paatero and Tapper (1994) and is now widely used for source apportionment around the world. Additional information about the model description is provided in the Supplement (Sect. S2).

In this study, 23 chemical species were used as input variables, namely OC, EC, ions (Na^+, NH_4^+, Mg^{2+}, Ca^{2+}, NO_3^-, SO_4^{2-}), trace metals (Al, Cu, Fe, Rb, Sb, Se, Sn, Ti, Zn), and organic markers (MSA, levoglucosan, polyols (sum of arabitol and mannitol)). We assumed that arabitol and mannitol came from a similar source and, hence, combined them into one component named "polyols" (Samaké et al., 2019). The uncertainties of the input variables were calculated based on Gianini et al. (2012). Finally, the species displaying a signal-to-noise ratio (S/N) lower than 0.2 were discarded, and those with S/N between 0.2 and 2 were classified as "weak", consequently multiplying the uncertainties by a factor 3.

2.4.2 Criteria for a valid solution

Solutions with a total number of factors from 6 to 11 were tested for the baseline models. Following the recommendations of the European guide on air pollution source apportionment with receptor models (Belis, 2019), the Q/Q_{exp} ratio (< 1.5), the geochemical interpretation of the factors, the weighted residual distribution, and the total reconstructed mass were evaluated during factor selection.

Moreover, the bootstrapping method (BS) was used on the final solution to estimate errors and ensure the stability and accuracy of the solutions. The BS method was applied with 100 iterations of the model, and contribution uncertainties are presented in the Supplement (Sect. S3) as mean $\pm$ SD of the 100 BS runs. The contribution uncertainties were estimated based on the method presented in Weber et al. (2019) and presented in Figs. S2 to S10. The daily species contributions are estimated using

$$X_{BSi} = G_{ref} \times F_{BSi},$$

where F_{BSi} is the profile of the bootstrap i, and X_{BSi} is the time series of each species according the reference contribution G_{ref} and the bootstrap run F_{BSi}.

Finally, the factor chemical profiles obtained during this study were compared with those from previous studies in France, using the PD-SID (Pearson distance–similarity identity distance) method (Belis, 2019; Weber et al., 2019), in order to validate their proper similarity.

2.4.3 Appropriate constraints in the PMF model

A set of constraints were applied on a basic model solution, in order to refine the results of the mathematical model by providing sound geochemical knowledge. Hence, the usual constraints as discussed in Weber et al. (2019), and some constraints corresponding to the traffic source following Charron et al. (2019) were also tested on the model (Table S3). However, these set of constraints were tested with caution as most of them have been previously applied only on sites with different typologies (i.e. urban or roadside sites), questioning their applicability in a rural site such as the OPE site. Finally, only a limited set was applied to generate the final solution (Sect. S1). After application of the constraints, a BS method was re-applied to verify the stability of the model.

2.4.4 Similarity assessment of chemical profiles

To investigate further any differences in the chemical profiles at the OPE site compared to those obtained at other French sites, a test of similarity was performed using the Pearson distance (PD) and standardized identity distance (SID) metric. This is calculated using Eqs. (S5) and (S6) in the Supplement (Sect. S2) (Belis et al., 2015), closely following a previous work by our group (Weber et al., 2019). This comparison is based on the source relative mass composition, which allows for the evaluation of the variability of PMF solutions across different sites. In this case, the chemical profiles obtained for the OPE site were compared against 15 different other sites over France. A "homogenous source" tends to have a similar profile over different site types and should have $PD < 0.4$ and $SID < 1.0$ (Pernigotti and Belis, 2018). Conversely, the sources with PD and SD values outside of this range are considered "heterogeneous sources".

2.5 OP source contribution estimation

The OP contribution of each PM_{10} source was determined by performing an OP deconvolution method using multiple linear regression (MLR) analysis. This methodology is based on the procedure proposed in Weber et al. (2018). Briefly, the OP activity (in nmol min^{-1} m^{-3}) was used as the dependent variable, while the PMF-resolved source PM_{10} mass contributions (in µg m^{-3}) are the independent variables, as shown in Eq. (1):

$$OP_{obs} = (G_n \times \beta_n) + \varepsilon, \quad (1)$$

where OP_{obs} is the observed daily OP_v (nmol min^{-1} m^{-3}) with matrix size $d \times 1$, G is the PMF-resolved source contribution (µg m^{-3}) of size $d \times n$, and β is the regression coefficient representative of the intrinsic OP (OP_m) (nmol min^{-1} μg^{-1}) of each n source. Finally, ε is the residual between the observed and modelled OP (nmol min^{-1} m^{-3}). The source-specific OP contribution is calculated by multiplying the regression coefficient of each source by the mass contribution of the source to PM_{10} ($G_k \times \beta_k$). This methodology is essentially based on that in Weber et al. (2018).

2.6 Season-trend (STL) deconvolution method

The STL (season-trend deconvolution using locally estimated scatterplot smoothing) model is a versatile and robust statistical method allowing for the decomposition of a time-series dataset into three components including trend, seasonality, and residual. The trend provides a general direction of the overall data; the seasonality is a repeating pattern that recurs over a fixed period of time; finally, the residual is the random fluctuation or unpredictable change in the dataset. The seasonal component allows us to eliminate seasonal variation from the time series, resulting in a smoothed trend line that shows the tendency of the time-series dataset. This method somehow takes into account the changes in seasonal cycles from year to year, which could also delineate part of the effect of meteorology on the long-term trend of PM_{10}.

To investigate the long-term trends of sources or species concentrations, the STL model (Cleveland et al., 1990) was applied on the monthly mean concentrations, as described by Eq. (2):

$$Y(t) = T(t) + S(t) + r(t), \quad (2)$$

where $Y(t)$ is the time series observed monthly on average, $T(t)$ is the trend component of the signal, $S(t)$ is the seasonal component, and $r(t)$ is the residual part not explained by the trend and seasonal part. The frequency was set to 13 (i.e. 6 months before and after the current month) to account for yearly seasonality. This model uses an iterative algorithm that constantly minimizes the residual $r(t)$ by successively adjusting the trend and seasonal components. It has to be noted that the resulting $T(t)$ and $S(t)$ do not represent concentrations but a statistical deconvolution of the input signal $Y(t)$. $S(t)$ could then be negative, and the trend $T(t)$ should be interpreted as an elaborated "moving average" of the concentrations. To account for extreme events or outliers in the data, the impact of data points with very high residuals was given less weight in the estimation of the trend and seasonal components, using the "robust" option of the algorithm. The presence and strength of tendency were evaluated thanks to the ordinary least-squares (OLS) linear fit of the $T(t)$ component against time, removing the first and last 6 months of the time series to avoid edge effects. Note that due to the lack of PM_{10} measurements in July 2019, the concentrations for that month were arbitrarily set to the August 2019 values.

This model was implemented in Python 3.8, making use of the "statsmodels" module (Seabold and Perktold, 2010).

3 Results and discussion

Section 3.1 to 3.5 below discuss the concentrations, sources, and trends of PM_{10}, while Sect. 3.6 and 3.7 discuss the OP measurements and sources.

3.1 PM_{10} and its major chemical components

The reconstructed mass of PM_{10} at the OPE site was calculated following Eq. (S1) in the Supplement and is presented in Fig. 2. The mass concentration of the reconstructed daily PM_{10} samples ranged from 2 to 51 $\mu g\,m^{-3}$, with an overall average of $9 \pm 7\,\mu g\,m^{-3}$ (median: $8\,\mu g\,m^{-3}$). This reconstructed PM_{10} mass concentration only exceeded the PM_{10} European limit value of $40\,\mu g\,m^{-3}$ a few times ($n = 3$) in the entire measurement period. These values are in the lower range of the concentrations reported for rural areas in Europe, ranging from 3 to 35 $\mu g\,m^{-3}$ (Putaud et al., 2004), and are relatively close to the values found at a remote site in Revin (France, located 165 km away), as described in the SOURCES programme (average of $13\,\mu g\,m^{-3}$) (Weber et al., 2019). Some changes in the concentration can be observed in the PM_{10} mass concentration, but there are no drastic changes in the major chemical components at the OPE, even with the lockdown restrictions during the year 2020. The yearly average volatile mass (i.e. unaccounted by chemical analysis), deduced from the difference between TEOM-FDMS (filter dynamics measurement system) measurements and reconstructed PM_{10}, ranges from 9 % to 44 % with an average of 22 % (of the yearly median) and is well within range generally found in a rural environment (Pey et al., 2009).

Accounting for 37 % to 45 % (based on year) of the reconstructed PM_{10} mass concentrations, organic matter (OM) is the largest contributor. The other main contributors are inorganic secondary species (NO_3^-, NH_4^+, non-sea-salt sulfate), suggesting a strong influence from LRT of pollutants. There are also contributions coming from dust and sea salt. Although all of these components are often dominated by specific emissions, they can be derived from a wide range of sources. For example, vehicular emissions are usually composed of both carbonaceous and metals species, while road dust is usually minerals and some metal species. Understanding the sources (as with the PMF methodology) and transformation processes of PM proves to be an essential step for efficient air quality policies.

3.2 Statistical stability of the PMF solution

The final retained solution includes nine factors as described in Sect. 3.3. Only 71 out of 100 baseline runs (without constraints) converged for this solution, but most factors were 100 % correctly mapped, except for the traffic factor (93 %, 66 out of 71 converged solutions) and sulfate-rich factor (99 %, 70 out of 71 converged solutions). Applying the constraints greatly improved the BS mapping to 100 % on all factors. Adding constraints in the base model allowed for refining of the model through addition of expert knowledge on the profiles, which led to the increased model stability. In previous source apportionment studies, specifically by our group, there are common constraints used depending on the site type such as presented in Borlaza et al. (2021a).

Particularly, the constraints for traffic-related factors reported in Charron et al. (2019) have been optimized for traffic and urban background sites in our previous works. However, these constraints appeared restrictive when applied in a rural typology such as the OPE site. In fact, the Cu-to-Sb ratios appeared unsuitable as this ratio was 6.3 in our final solution compared to 12.6 in Charron et al. (2019). Based on literature, the Cu-to-Sb ratio can range from 1.6 (Handler et al., 2008) to 12.6 (Charron et al., 2019) depending on site typology. The addition of this constraint resulted in or led to a non-convergent solution at the OPE site. To avoid inconsistencies, the Cu / Sb constraint was excluded in the optimal solution. The OC-to-EC ratio in the traffic profile was also too restrictive for the model, as this ratio was 3.9 in our baseline solution against 0.44 in Charron et al. (2019). The OC / EC levels calculated in this profile also suggest a strong influence of secondary organic aerosols (SOAs) (Johnson et al., 2006; Pio et al., 2011; Rodríguez González et al., 2003; Viana et al., 2006), instead of primary traffic emissions. As OC in a rural site can undergo multiple re-transformations in the atmosphere from the emissions sources, this has led to a wide range of OC-to-EC ratios as similarly found in Weber et al. (2019); hence this constraint was excluded.

In the final model, some constraints were used as summarized in Table S3, which resulted in all factors being correctly mapped and all BS runs converging, suggesting a good improvement in the traffic (from 93 % to 100 %) and sulfate-rich (from 99 % to 100 %) factors as well as the overall statistical robustness of the model. The other constraints either resulted in a non-convergent constrained model and/or less robust BS results. This implies that in sites with strong influence of LRT, the appropriate constraints tend to vary, and an optimal PMF solution can be more difficult to achieve.

The challenge in adding the constraints may also be linked to the inherent nature of the PMF algorithm since it assumes chemical profiles are identical for the whole period of analysis. However, during the 9 years of this study, some chemical source profiles may have changed, notably the traffic factor. Indeed, an evolution of the car fleet in France and Europe could lead to the changes in the OC-to-EC ratio emitted by the vehicle, so this profile may also have changed during this period. For this specific case, a rolling PMF approach (Canonaco et al., 2021) with a statistically mapped PMF profile could be useful to investigate the time variability of a given profile, slightly evolving with time.

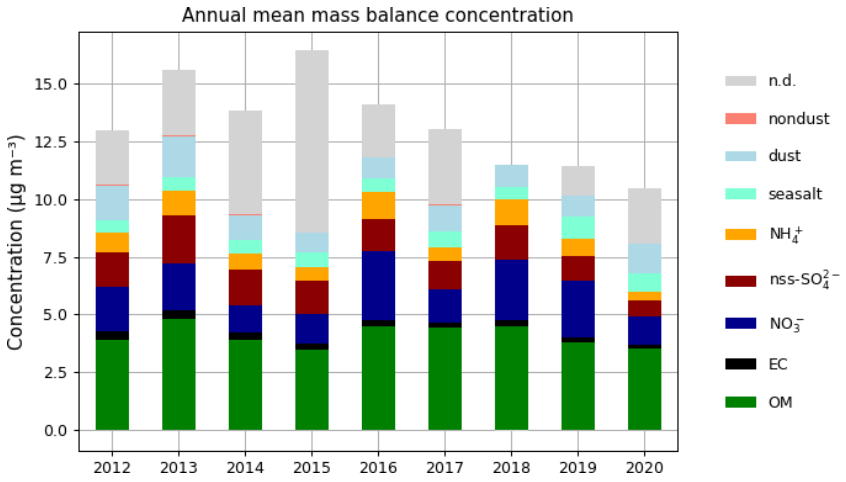

Figure 2. The annual average of PM_{10} composition at the OPE site.

3.3 PMF solution description and PM_{10} contributions

The nine resolved sources of PM_{10} at the OPE site include nitrate-rich (25 % of average contribution to PM_{10} for the full period), sulfate-rich (15 %), traffic (12 %), mineral dust (16 %), biomass burning (9 %), fresh sea salt (4 %), aged sea salt (6 %), primary biogenic (7 %), and MSA-rich (7 %). These factors were identified based on their chemical profiles and the mass loading of specific tracers, as summarized in Table S2 in the Supplement. The error estimations, chemical profiles, and temporal evolutions of the PMF-resolved sources are available in the Supplement (Sect. S3). Figure 3 represents the repartition of the chemical species in the different factors. The summed PM_{10} contributions from all sources showed very good mass closure ($r = 0.95$) with PM_{10} mass reconstructed with Eq. (S1), indicating very good model results.

The factors with highest average contribution to the PM_{10} mass are the two inorganic secondary aerosol sources, nitrate-rich (25 %, $2.3 \pm 4.3\,\mu g\,m^{-3}$) and sulfate-rich (15 %, $1.4 \pm 1.5\,\mu g\,m^{-3}$), and mineral dust (16 %, $1.6 \pm 1.7\,\mu g\,m^{-3}$). Sulfates and nitrates are mainly formed through secondary processes in the atmosphere with long atmospheric lifetimes and can, therefore, originate from regional sources or LRT. Considering the agriculture and natural emissions of ammonia, especially expected in a rural site, secondary aerosols could also be formed locally at the OPE site. The less dominant sources are traffic, biomass burning, biogenic (MSA-rich, primary biogenic), and sea salts (fresh and aged). The contributions of the different factors are quite similar to those observed at other rural sites in France (Weber et al., 2019).

The OPE site has a Northern Hemisphere mid-latitude climate with four seasons, (1) a winter season corresponding to the months of December, January, and February; (2) a spring season corresponding to March, April, and May; (3) a summer season corresponding to June, July, and August; and (4) a fall season corresponding to September, October, and November. Seasonality in some factors can be apparent, such as for the biomass burning and nitrate-rich factors, which are more prominent in winter and spring, respectively, and the primary biogenic and MSA-rich factors, increasing in summer due to greater photochemical and biological activities. Figure 4 depicts the seasonal average contributions of the PM_{10} sources at the OPE site from the year 2012 to 2020.

The *nitrate-rich* factor, identified by high loadings of NO_3^- and NH_4^+, has a strong seasonal pattern with a maximum contribution to PM_{10} mass concentration, especially in the months of March and April.

The *sulfate-rich* factor is identified by high loadings of SO_4^{2-} and NH_4^+. There are also contributions from some metal species (Se, Zn, Cu, and Sb) in this factor, suggesting potential influence from road dust and/or non-tailpipe vehicular emissions. A small portion of OC (5 % of OC mass) is also observed in this factor. The presence of these metals remained, even when the number of factors was increased (up to 11 factors) during the PMF optimization process.

The *aged sea salt* factor is characterized by high loadings of Na^+ and Mg^{2+}, with a certain number of species originating from potentially anthropogenic sources such as nitrates (6 % of NO_3^- mass) and sulfates (19 % of SO_4^{2-} mass) that can be attributed to mixing and transformation processes in the atmosphere. Interestingly, there are some contributions from EC (8 % of EC mass), Cu (11 % of Cu mass), Sb (13 % of Sb mass), and Se (19 % of Se mass). This could imply potential mixing of aged sea salt with other anthropogenic source linked to these species (e.g. traffic, shipping). The minimal loadings observed in the contributions of Cl^- in this factor could likely be the result of ageing processes occurring between sea salt and acidic particulate compounds such as nitric and sulfuric acid (Seinfeld and Pandis, 2016). This factor could also be associated with road salting in the winter; however there is no clear seasonality in the contributions

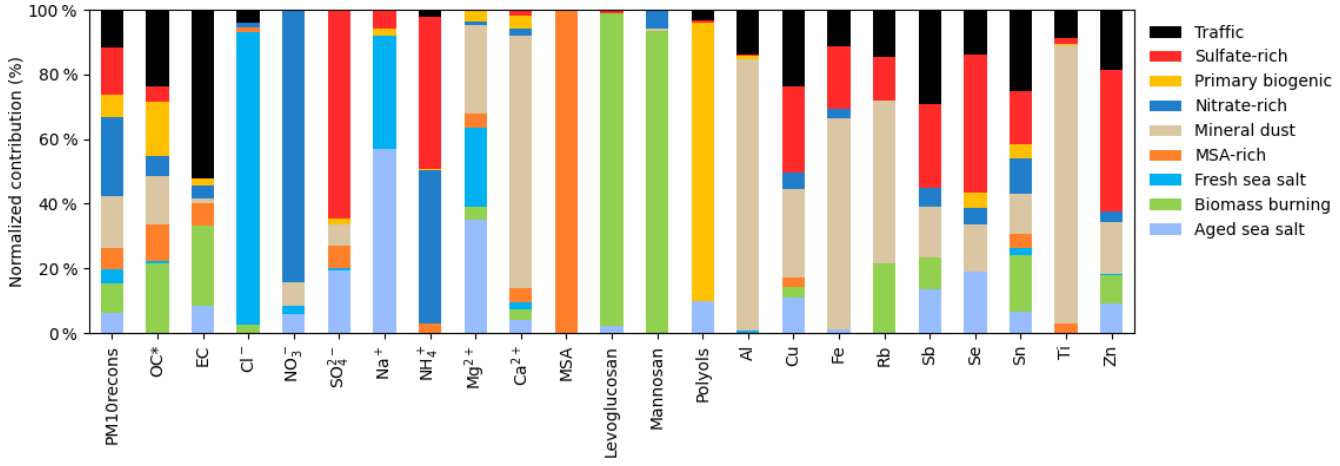

Figure 3. Species repartition by PMF-resolved sources at the OPE site.

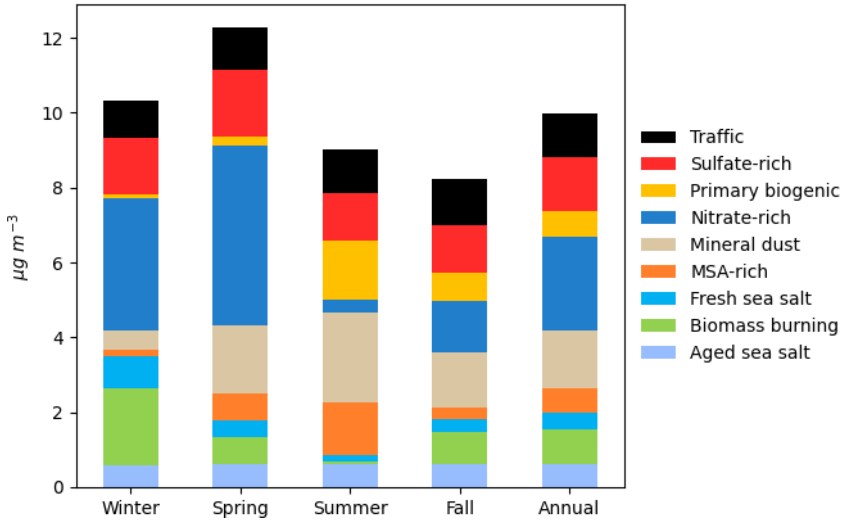

Figure 4. Seasonal and annual contribution of the PMF-resolved sources at the OPE site.

to support this hypothesis. There was no added constraint in this factor as our solution shows a Mg^{2+}/Na^{+} ratio at 0.06, while this ratio is usually found to be around 0.12 in sea salt emissions (Henderson and Henderson, 2010).

The *fresh sea salt* factor is characterized by high loadings of Cl^{-} (91 % of Cl^{-} mass) and some contributions from Na^{+} (35 % of Na^{+} mass) and Mg^{2+} (25 % of Mg^{2+} mass). This factor contributes 4 % to total PM_{10} mass, and, unlike the aged sea salt factor, it is less likely influenced by anthropogenic sources with extremely low contributions from carbonaceous and metal species.

The *MSA-rich* factor is identified by high loadings of MSA (methanesulfonic acid), a known product of oxidation of dimethylsulfide (DMS), commonly from marine phytoplankton emissions (Chen et al., 2018; Li et al., 1993). A small mass fraction of SO_4^{2-} (7 % of SO_4^{2-} mass) is also found in this factor that may be due to the co-emission of DMS and non-sea-salt sulfates but also results from the production of biogenic sulfate from DMS oxidation. Hence, MSA-rich sources could potentially be mixed with secondary inorganic aerosols as well. The measured MSA mass concentration showed weak correlations with specific ionic species from marine aerosols such as Na^{+} ($r < 0.01$) and Mg^{2+} ($r < 0.01$). This could indicate that marine biogenic emissions may not be the only source of this factor. Instead, this factor could be influenced by sources with terrestrial origins and/or from forest biota, as previously reported in other studies (Bozzetti et al., 2017; Golly et al., 2019; Jardine et al., 2015; Miyazaki et al., 2012). This factor also presents a clear seasonal pattern with maximum contribution from May to July due to higher photochemical activity and algae/microbial activity. Golly et al. (2019) reported a very coherent seasonal cycle for MSA concentrations over a large portion of the French territory, including at the OPE site.

The *primary biogenic* factor is characterized entirely by polyols. These species are emitted by fungal spores which partly explains the high loadings of OC found in this factor. This factor has a higher contribution to PM_{10} during the summer season, consistent with the observations at other rural and urban sites (Samaké et al., 2019; Weber et al., 2019; Borlaza et al., 2021a). More details about the characteristics of primary biogenic aerosols can be found in Samaké et al. (2019). Briefly, meteorological conditions, such as high temperature and relative humidity, could facilitate the increase in their formation. This factor can also include some fraction of plant debris, identified by cellulose measurements, as discussed in Samaké et al. (2019), Borlaza et al. (2021a), and Brighty et al. (2022).

The *biomass burning* factor, a major contributor to PM_{10} during the winter season, includes mostly levoglucosan and mannosan. This factor contains around 25 % of the total EC mass, consistent with a combustion chemical profile. Trace elements like Rb and Sn are also found in this factor, rubidium being the major trace element with 21 % of its mass being reconstructed in this factor. Due to the distance of any residential areas from the OPE site, the contributions of this factor to PM_{10} at 20 % on average in winter are much less than the contributions generally observed in most sites in France in winter (e.g. urban, suburban, or countryside sites; Zhang et al., 2020), which are mainly in the range of 25 %–70 %, with an average of about 35 % (Weber et al., 2019). The contribution at the OPE site most probably represents the average winter loading of the French national background of the atmosphere.

The *traffic* factor is the second factor where EC is a major contributor (52 % of EC mass). The major trace elements found in the traffic factor are Cu, Sb, Sn, and Zn, and most of their masses are reconstructed in this factor. There is no seasonality associated with this factor. However, its contribution to PM_{10} presents a decreasing trend over the sampling period from 2012 to 2020. This is also consistent with the decreasing trend found in EC mass concentrations over the same period, as presented in Fig. S11. These findings present an opportunity to explore the potential decrease in traffic emissions observed at the OPE site, taken as a good proxy of the national background burden of the rural atmosphere. This is further discussed in Sect. 3.5.

The *mineral dust* factor is mainly composed of Ca^{2+} (78 % of Ca^{2+} mass), Al (84 % of Al mass), and Ti (86 % of Ti mass). There are also contributions from other trace elements that could originate from re-suspended road dust or non-tailpipe emissions such as Fe (65 % of Fe mass), Cu (27 % of Cu mass), Rb (51 % of Rb mass), and Zn (16 % of Zn mass). A fraction of it could therefore be of anthropogenic origin.

3.4 Comparison of the source chemical profiles with previous results in France

Figure 5 presents the similarity plot (PD-SID distances) obtained for the nine factors found at the OPE site compared to the French sites included in the SOURCES programme (Weber et al., 2019). It is striking that most factors remained homogeneous within France, including both rural and urban sites. The most stable factors are nitrate-rich (lowest PD) and mineral dust (lowest SID). The traffic factor also appears relatively stable but presents some dissimilarities according to the high variation in the PD metric. A high PD variation generally indicates a difference in the chemical species that identify the main mass contribution of the profile. In fact, in the traffic factor, this variation between the OPE and other sites can be attributed to the variations in the OC to EC levels, similar to the findings in Weber et al. (2019). Compared to the other French sites, the OC to EC levels of this factor at the OPE site are much higher, which highlights a strong influence from LRT processes with SOA formation.

The aged sea salt and MSA-rich factors are the only ones positioned outside of the shaded box in Fig. 5, indicative of heterogeneous profiles between the OPE and the other sites. The heterogeneity found in the aged sea salt profile can be attributed to the contributions of EC and some metals in this factor. These were not typically found in other sites in France and could also be due to the mixing of this sea salt profile with other anthropogenic contributions as a result of LRT processes, as well as different ageing processes. Similarly, the MSA-rich factor has previously shown site-to-site variations and a wide variation in the PD-SID metric (Weber et al., 2019), mostly attributed to the variability of the contribution of OC in some sites. This is also the case at the OPE site, with a large contribution of about 11 % of OC in this MSA-rich factor. Despite these few differences, the very large similarity of the chemical profiles at OPE compared to those at all other sites in France will be essential to the comparison of the intrinsic OP of sources in Sect. 3.7.

3.5 Long-term trends of PM_{10} sources

Figure S10 in the Supplement presents the long-term trend of the observed PM_{10} at the OPE site. The PM_{10} levels appear to be consistent from 2012 to 2020, and there is no clear increasing or decreasing trend found in PM_{10} ($r^2 = 0.2$, Table 1). However, there is a clear decline found in EC mass concentrations ($r^2 = 0.9$), with a reduction of 22 ng m^{-3} yr^{-1} ($p \leq 0.01$) (Fig. S11 in the Supplement). This could indicate that the mass contribution of one or more sources contributing to EC should also be decreasing. Following Germany and Italy, France is placed third on highly impacted countries in Europe from vehicular exhaust emissions (Anenberg et al., 2010). Through the years, a variety of vehicular regulations have been adopted to reduce traffic-related emissions, not only in France (Bernard et al., 2020), but also across Eu-

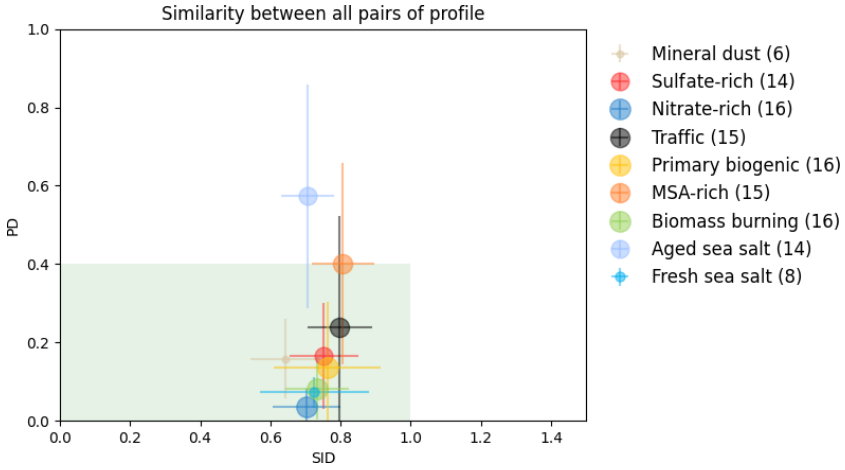

Figure 5. Similarity plot of the OPE site against all the French sites in the SOURCES programme. The shaded area (in green) shows the acceptable range of the PD-SID metric. For each point, the error bars represent the standard deviation in the comparisons of all pairs of sites. The number in the legend indicates the number of sites over France where the given profile is available.

Table 1. STL tendencies of the observed PM_{10} and each PMF-resolved source contributions to PM_{10} from the year 2012 to 2020 at the OPE site.

	Tendency ($\mu g\,m^{-3}\,yr^{-1}$)	r^2	p value
Observed PM_{10}	−0.107	0.21	≤ 0.01
EC	−0.022	0.89	≤ 0.01
Traffic	−0.104	0.67	≤ 0.01
Aged sea salt	−0.042	0.52	≤ 0.01
Fresh sea salt	0.052	0.77	≤ 0.01
Mineral dust	−0.055	0.09	≤ 0.01
MSA-rich	0.013	0.14	≤ 0.01
Nitrate-rich	−0.002	0.00	0.90
Primary biogenic	−0.027	0.82	≤ 0.01
Sulfate-rich	−0.072	0.57	≤ 0.01
Biomass burning	−0.033	0.64	≤ 0.01

rope (Wappelhorst and Muncrief, 2019). The data obtained at the OPE site present an interesting opportunity as they cover 9 years of sampling in a rural area, making it possible to investigate emission trends over a long period of time in a site representing a background atmosphere.

Using the model described in Sect. 2.6 (Eq. 2), the STL deconvolution of the PMF-resolved sources at the OPE site was also investigated. It is extremely significant that the contributions from the traffic factor at the OPE site also decreased substantially, as presented in Fig. 6. A very large reduction of 58 % from the year 2012 to 2020 based on average mass contribution and an overall yearly average reduction of $104\,ng\,m^{-3}\,yr^{-1}$ ($p \leq 0.01$) were found. In parallel, there is also a reduction observed in the sulfate-rich factor, proposed as a highly anthropogenic-derived factor (see Fig. S12 in the Supplement), with 66 % reduction of average mass contribution and an overall yearly average reduction of $72\,ng\,m^{-3}\,yr^{-1}$ ($p \leq 0.01$). Indeed, several other sources have shown lower but significant decrease of their mass contribution over the years (Table 1) at the OPE site, except for the fresh sea salt, nitrate-rich, and MSA-rich factors.

These findings allowed for the unravelling of the decreasing trend in terms of source contributions by the STL model. The STL deconvolution was applied on all the identified sources, which clearly showed that the traffic source has the highest tendency with a decreasing trend. The other major sources of PM, such as biomass burning, mineral dust, and nitrate-rich sources, do not have as much decreasing tendency as the traffic factor. The internal annual variabilities of weather/climate conditions might not be the leading factors explaining these trends, as they would have affected PM sources in the same way.

The downward trends found in our study are very consistent with other existing studies in Europe (Li et al., 2018; Sun et al., 2020; Salvador et al., 2012; Pandolfi et al., 2016; Gama et al., 2018; Amato et al., 2014), with nearly all of them conducted in urban areas. Pandolfi et al. (2016) found a significant long-term decrease of the contributions from anthropogenic emissions (specifically a mixed industrial/traffic factor, $-0.11\,\mu g\,m^{-3}\,yr^{-1}$, 56 % total reduction) in a regional background site in altitude in the northeast of Spain (Montseny, Spain) from 2004 to 2014. This is also consistent with a similar study in the metropolitan area of Madrid, Spain (Salvador et al., 2012), which showed a reduction of 32.7 % attributed to traffic emissions, alongside the decrease of the carbonaceous and SO_4^{2-} in PM. In a southern Spain area (Andalusia), the same group also found a consistent decreasing trend of PM at some traffic and urban sites in the region (Amato et al., 2014).

Another long-term study in central Europe (Sun et al., 2020) focusing on equivalent black carbon (eBC) concen-

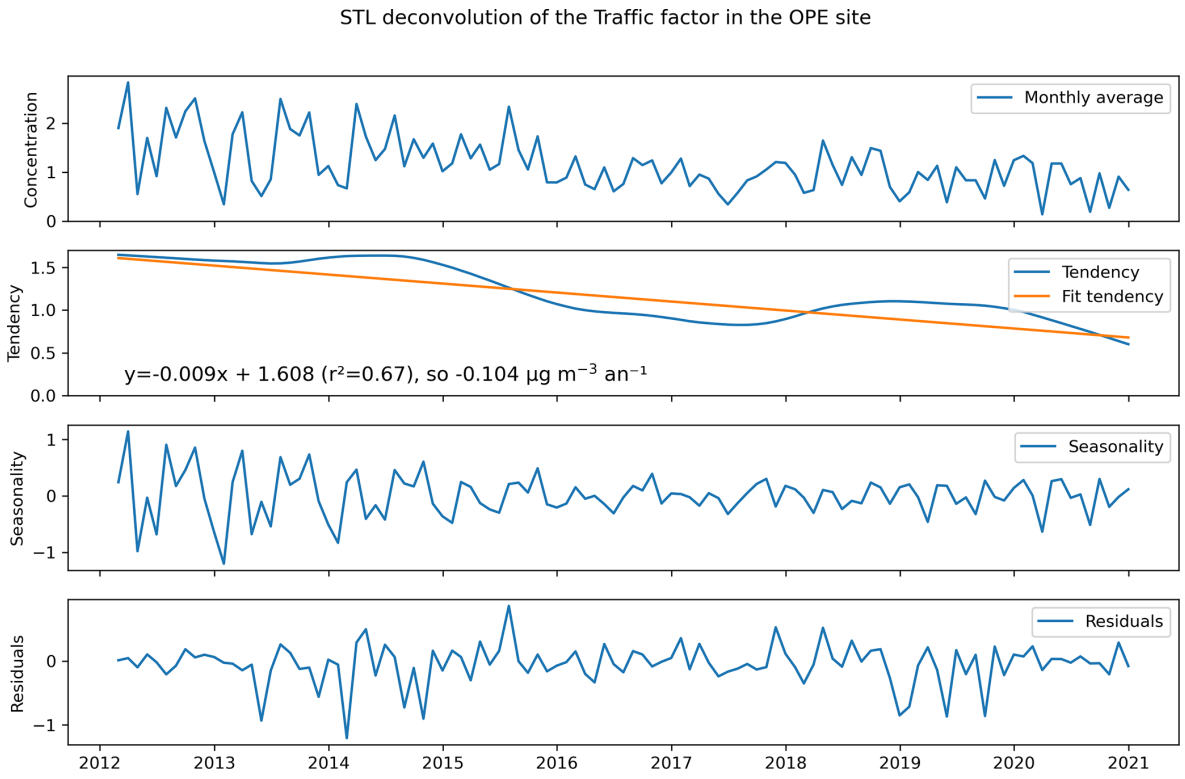

Figure 6. The season-trend (STL) deconvolution of contributions (in $\mu g\,m^{-3}$) from the traffic factor to PM_{10} from the year 2012 to 2020.

trations found decreasing trends in high-altitude Alpine sites located in Germany ($-3.88\,\%\,yr^{-1}$, $[-10.15\,\%, 0.56\,\%]$) and Switzerland ($-3.36\,\%\,yr^{-1}$, $[-8.71\,\%, -0.28\,\%]$). These findings are also consistent with results from other parts of Europe, with the largest decrease found in OC up to $-48\,\%$ (Cusack et al., 2012), and the decrease in PM has been associated with non-meteorological factors (Barmpadimos et al., 2012). Other studies with pluri-annual series of data on PM chemistry in rural environments in Europe include Spindler et al. (2013) (Melpitz, Germany, including EC measurement for 2003–2011) and Grange et al. (2021) (Payerne, Switzerland, comparison of three periods every 10 years since 1998, including EC and trace elements). Both show a decrease in EC concentrations over time during the study. Finally, while these studies did not target specific chemical species solely linked to vehicular emissions, most of them attributed the decline to the efforts to reduce vehicular emissions and other mitigation policies in their respective areas.

It should be noted that the role of meteorology in the observed decrease in PM in these studies (including ours) cannot be totally ruled out (Hou and Wu, 2016; Czernecki et al., 2017; Kim, 2019) and is generally not fully considered. In most cases, there is a complex interplay between PM and meteorological conditions that could increase or decrease PM mass concentration (Chen et al., 2020). Indeed, there are some studies at high-altitude or regional background sites that highlighted a concurrent role of changing meteorology and changes in frequency of Saharan dust advection to Europe (Brattich et al., 2020) in modulating the dust concentrations in the atmosphere. The study at Melpitz (Spindler et al., 2013), despite an in-depth work on the wind sector classification, does not address the impact of possible changing in the air mass origin on long-term changing origins.

The evolution of the absolute concentration of the traffic factor (in $\mu g\,m^{-3}$) at the OPE site was also compared to an evaluation of black carbon (BC) emissions (in kilotonnes) by the transport sector for overall France, provided by the CITEPA, the official agency in charge of the emissions inventory in France (https://www.citepa.org/fr/2021-bc/, last access: 5 July 2022). Both series were converted to an arbitrary level starting from 100, using 2012 as the base year (Fig. 7). This figure shows an excellent agreement in the trend and in the total percentage decrease (%) for estimated BC emissions from traffic ($-64\,\%$) and the traffic source contributions observed at the OPE site ($-52\,\%$), between the years 2012 to 2020. While local or regional changes in meteorology may be a factor in the evolution of the concentrations observed, this is unlikely to be the dominant one in the evolution of the concentrations of chemical species related to traffic emissions, in light of the strong correlation observed with the national emissions inventory in France.

The interesting point of our study is that it pertains directly to a specific source, identified with a long-term and robust PMF study. Further, as there are minimal local anthro-

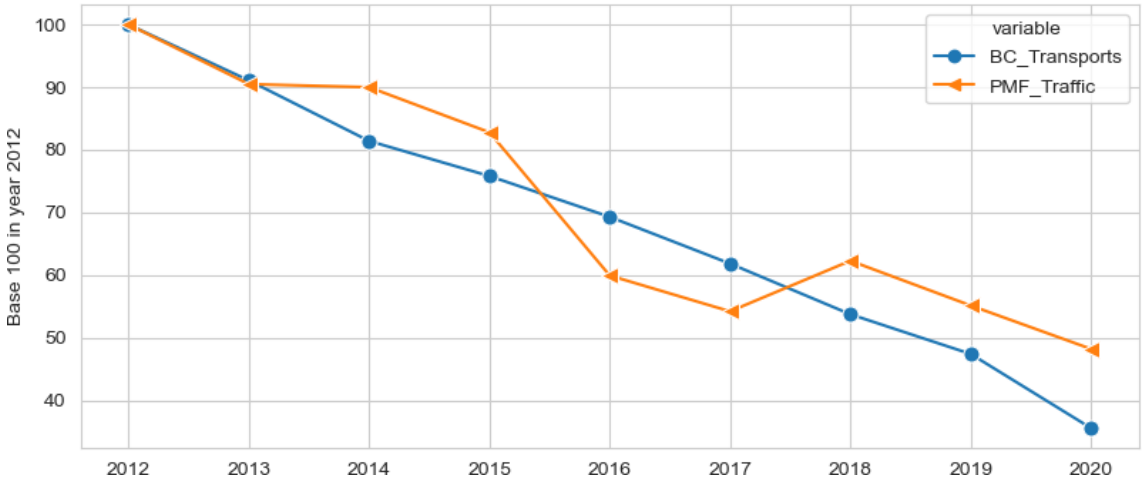

Figure 7. Comparison of the evolution of the traffic factor source contribution (in $\mu g\,m^{-3}$) at the OPE site and the black carbon (BC) emissions (in kilotonnes) by the transport sector (source: CITEPA, https://www.citepa.org/fr/2021-bc/) for overall France.

pogenic sources expected at the OPE site, it may be safe to assume that these contributions to PM mass in this area are influenced by LRT of pollutants. Our results indicate that the implementation of emission control policies is also playing a role in the consistent decrease in traffic emissions in rural sites far away from direct emissions.

3.6 Temporal trends of observed OP of PM_{10}

Figure 8 presents the observed average values of OP of PM_{10} at the OPE site compared to the other sites in France (Calas et al., 2018, 2019; Weber et al., 2021, 2018). All series cover at least 1 year of sampling. As expected, the OP level in a rural background is much lower (about 2 to 8 times) than other typologies including traffic, urban, and urban alpine sites, for both AA and DTT assays. Further, the average ratio between urban sites and the rural OPE site is generally much higher for OP than for PM mass, an indication that the nature of the particles at the rural site makes them less oxidant than in urban areas, as already pointed out in Daellenbach et al. (2020).

Figure 9 presents the daily and monthly mean distributions of observed PM_{10} and OP activity (OP_v^{DTT} and OP_v^{AA}) from 13 June 2017 to 22 December 2020. There is an observed seasonality, where PM_{10} and OP_v^{DTT} appear to be similar with relatively higher levels during warmer months. On the contrary, OP_v^{AA} has slightly higher levels during colder months.

In many European studies, the seasonality in PM_{10} mass concentration can be usually explained by higher contributions from biomass burning during winter (Bessagnet et al., 2020; Tomaz et al., 2017), especially in alpine valleys (Calas et al., 2019; Favez et al., 2010; Herich et al., 2014; Srivastava et al., 2018; Tomaz et al., 2016, 2017; Weber et al., 2018, 2019; Borlaza et al., 2021a). Similarly, this seasonal pattern has been observed in OP as well (Borlaza et al., 2021b; Weber et al., 2018; Calas et al., 2019; Weber et al., 2021). However, the typology (i.e. rural) of the OPE site could be associated with a different type of OP temporal profile as it is far from direct anthropogenic emission sources (but not from vegetation and soil biogenic emissions).

With the large influence of LRT on the sources of PM at the OPE site, this also poses an opportunity to investigate the impact of LRT on OP. In fact, few studies have looked into the effects of aerosol ageing on OP properties (Guascito et al., 2021; Bates et al., 2019). Pietrogrande et al. (2019) reported association of OP with redox-active organics linked to photo-oxidative ageing. Using backward trajectory analysis, Wang et al. (2020) found strong effects of LRT on OP of fine PM. This is also consistent with the findings in Paraskevopoulou et al. (2019), which revealed highly oxygenated secondary aerosols as one of the main drivers of OP in fine PM, further highlighting the importance of combustion and ageing processes in OP. In a shipborne measurement study in South Korea, a higher intrinsic OP has also been found in samples where secondary aerosol formation is more dominant, also suggesting the strong impacts of long-range transported PM (Oh et al., 2021). Cesari et al. (2019) found negligible contribution from secondary sulfates but have found relevant OP contributions from a factor identified as a combination of vehicular traffic and secondary nitrates. All these studies used DTT assays to measure the OP of PM.

The OP assay sensitivity to specific species and/or sources can also explain the difference in seasonality found in OP_v^{DTT} and OP_v^{AA} in our study. OP_v^{DTT} appears sensitive towards organics, metals, and, possibly, a synergistic effect between the two (Bates et al., 2019; Dou et al., 2015; Fang et al., 2017; Gao et al., 2020b, a; Jiang et al., 2019; Weber et al., 2021; Yu et al., 2018; Borlaza et al., 2021b), while OP_v^{AA} shows sensitivity mostly towards metal species (Bates et al., 2019;

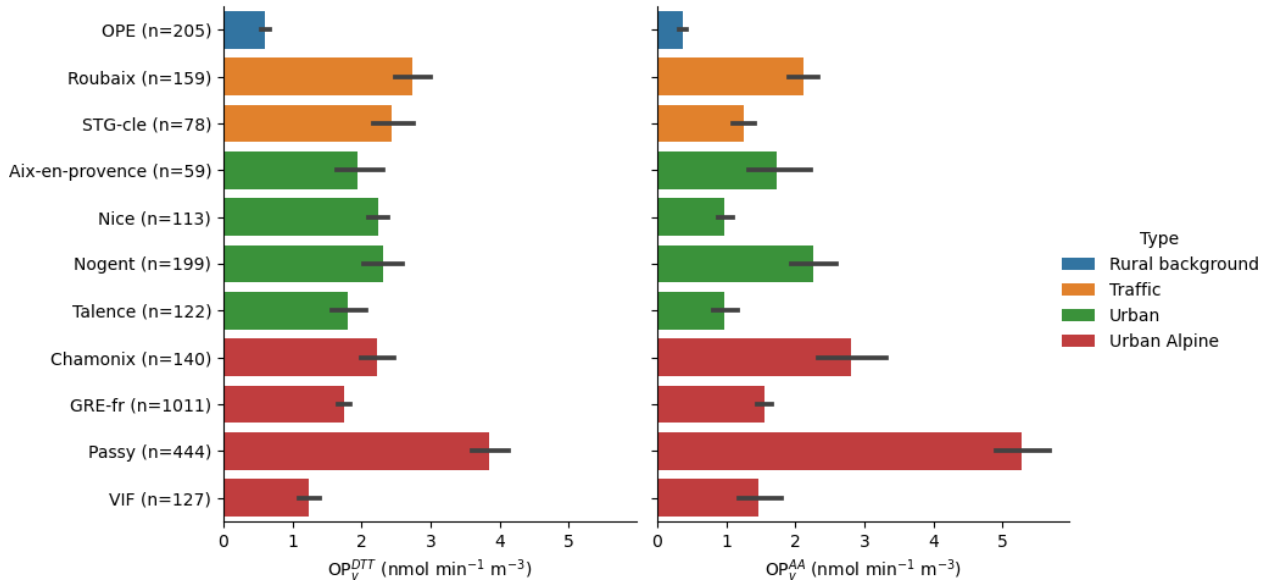

Figure 8. The comparison of observed OP activity (OP_v^{DTT} and OP_v^{AA}) between the OPE site and other sites in France. Bar plots depict the mean value with standard deviation.

Figure 9. Temporal distributions of observed PM_{10} and OP activity (OP_v^{DTT} and OP_v^{AA}) from the year 2017 to 2020 at the OPE site in terms of daily and monthly mean.

Crobeddu et al., 2017; Visentin et al., 2016; Weber et al., 2021; Borlaza et al., 2021b).

Generally, current literature shows importance of the role of secondary/aged aerosols in the OP of PM, especially those with influence from anthropogenic sources. However, to our knowledge, this is the first long-term OP study that specifically deals with ambient samples far from direct emissions at a rural background site.

3.7 Sources of OP in PM_{10}

The sources of OP in PM_{10} were apportioned following an OP deconvolution method proposed by Weber et al. (2018) using the source contributions ($\mu g\,m^{-3}$) obtained in the PMF and the measured OP ($nmol\,min^{-1}\,m^{-3}$) at the OPE site. Generally, the modelled OP (OP_m) is within range of the observed OP, with a reasonable reconstruction (OP_v^{DTT} ($r = 0.76$) and OP_v^{AA} ($r = 0.76$)). The OP_m of each PM source is given in Table 2, where OP_m^{DTT} can range from -0.01 ± 0.02 to $0.10 \pm 0.03\,nmol\,min^{-1}\,\mu g^{-1}$, and OP_m^{AA} can range from -0.001 ± 0.02 to $0.16 \pm 0.03\,nmol\,min^{-1}\,\mu g^{-1}$. Generally, higher OP_m indicates higher redox activity associated with the factor. There are some differences in the OP_m based on the type of assay used, and this can be attributed to the sensitivity of the assay towards certain redox-active species in PM (Borlaza et al., 2021b; Xiong et al., 2017; Charrier and Anastasio, 2012).

In terms of overall daily mean contribution, as presented in Fig. 10, the main contributors to PM_{10} mass are the nitrate-rich, mineral dust, and sulfate-rich factors at the OPE site. However, in terms of OP_v^{DTT}, the mineral dust factor showed the highest average contribution ($0.15\,nmol\,min^{-1}\,m^{-3}$), followed by the sulfate-rich ($0.11\,nmol\,min^{-1}\,m^{-3}$) and traffic ($0.07\,nmol\,min^{-1}\,m^{-3}$) factors. For OP_v^{AA}, the biomass burning factor showed the highest contribution ($0.12\,nmol\,min^{-1}\,m^{-3}$), followed by the traffic ($0.07\,nmol\,min^{-1}\,m^{-3}$) and nitrate-rich ($0.06\,nmol\,min^{-1}\,m^{-3}$) factors.

Although lower in magnitude, the OP contribution of mineral dust, traffic, and biomass burning (only in OP_v^{AA}) is also prominent at the OPE site, similar to other sites in France (Weber et al., 2021). These sources are commonly composed of species that are highly redox-active; hence it is not surprising that they are one of the main drivers of OP, even in a rural site. Both mineral dust and biomass burning are also sources that can be associated with LRT and ageing, respectively, which are atmospheric processes linked to increased OP (Pietrogrande et al., 2019; Wang et al., 2020; Paraskevopoulou et al., 2019; Oh et al., 2021). Further, while the mineral dust profile in OPE is considered homogeneous with those determined in other parts of France, as discussed above, its chemical composition includes slightly larger fractions of some metals, particularly Fe and Cu, possibly making it more redox-active.

As observed in other studies (Daellenbach et al., 2020; Borlaza et al., 2021b; Weber et al., 2021), there is also a clear difference in source ranking when considering the PM mass or OP, highlighting that the sources driving PM mass are not the same as the ones driving OP activity. The mass contributions of the nitrate-rich factor can be twice those of the traffic factor. However, in terms of OP (both OP_v^{DTT} and OP_v^{AA}), the traffic factor contribution can be twice as much as that of the nitrate-rich factor. The biomass burning factor, with only $< 1\,\mu g\,m^{-3}$ mass contribution on annual average, appears to have the highest contribution in OP_v^{AA}.

Some previous studies associated secondary inorganic aerosol (SIA) sources with minimal contributions on PM toxicity (Cassee et al., 2013; Daellenbach et al., 2020; Park et al., 2018). However, the nitrate-rich factor apportioned at the OPE site showed contributions to both OP_v^{DTT} and OP_v^{AA} and the sulfate-rich factor to OP_v^{DTT}. In the sulfate-rich factor, a fraction of OC (5 %) and metals (Se (42 %), Zn (44 %), Cu (27 %), and Sb (25 %)) were apportioned, while in the nitrate-rich factor there are contributions from OC (6 %), EC (4 %), and metals (Sb (6 %) and Sn (11 %)). These species are commonly anthropogenic-derived, signalling that the sulfate- and nitrate-rich factors could be influenced by these types of emissions as well. In fact, a similar study considered that both SIA factors can be associated with anthropogenic SOA sources (Borlaza et al., 2021a).

Although both DTT and AA assays represent potential PM-induced oxidative stress, through in vivo interactions between redox-active components in PM_{10} and biological oxidants, it can be observed that they differ in terms of source impacts. This can be attributed to the sensitivity of each assay to specific species and/or emission sources of PM. Nevertheless, most of the sources of PM suggested to be anthropogenic-derived or impacted, such as traffic, mineral dust, nitrate-rich, sulfate-rich (only in OP_v^{DTT}), and biomass burning (only in OP_v^{AA}), were all usually on the upper half of the scale (Fig. 8) in terms of OP_v contributions. The knowledge of source-specific OP_v contributions provides useful information on the main drivers of OP_v, even in a rural area such as the OPE site.

There is an interesting seasonality observed in the OP of PM, as previously shown in Fig. 9. With the OP source deconvolution method, this seasonality has been revealed in terms of PM sources, as presented in Fig. 11. During colder months, the biomass burning factor clearly dominated the OP_v^{AA} contributions. During warmer months, the OP_v^{DTT} contributions were dominated by the mineral dust factor. However, there is a relatively consistent monthly contribution for both assays coming from the traffic factor.

It is also interesting to note the negative contributions from some sources. This negative contribution is brought by a negative intrinsic OP (OP_m obtained in the OP deconvolution method; Table 2). This can be broadly interpreted as follows: for every $1\,\mu g\,m^{-3}$ increase in the MSA-rich factor, there is an associated decrease in OP_v^{AA} contributions ($OP_m = -0.06 \pm 0.03$, $p = 0.06$). A similar interpretation can be done for the primary biogenic factor and its OP_v^{DTT} contributions ($OP_m = -0.01 \pm 0.02$, $p = 0.68$). However, it is important to note that both MSA-rich and primary biogenic factors do not always present a negative OP_m at every site investigated in our group. One cannot completely assume that these two factors always act as suppressors of OP of PM. In fact, these two factors have shown high OP_mvariabilities across different sites in France (We-

Table 2. Regression coefficients (i.e. intrinsic OP or OP_m, expressed in nmol min^{-1} μg^{-1}) at the OPE site for the DTT and AA assays. The values are the mean ± standard deviation, and the p value is in the parentheses.

Factor	OP_m^{DTT}	OP_m^{AA}
Traffic	0.07 ± 0.04 ($p = 0.09$)	0.08 ± 0.01 ($p \leq 0.01$)
Aged sea salt	0.06 ± 0.04 ($p = 0.20$)	0.08 ± 0.04 ($p \leq 0.05$)
Fresh sea salt	0.02 ± 0.02 ($p = 0.40$)	0.02 ± 0.02 ($p = 0.22$)
Mineral dust	0.10 ± 0.03 ($p \leq 0.01$)	0.04 ± 0.01 ($p \leq 0.01$)
MSA-rich	0.04 ± 0.04 ($p = 0.21$)	-0.06 ± 0.03 ($p = 0.06$)
Nitrate-rich	0.01 ± 0.01 ($p = 0.10$)	0.03 ± 0.01 ($p \leq 0.01$)
Primary biogenic	-0.01 ± 0.02 ($p = 0.68$)	-0.005 ± 0.01 ($p = 0.82$)
Sulfate-rich	0.10 ± 0.03 ($p \leq 0.01$)	-0.001 ± 0.02 ($p = 0.98$)
Biomass burning	0.03 ± 0.03 ($p = 0.42$)	0.16 ± 0.03 ($p \leq 0.01$)
Intercept (nmol min^{-1} m^{-3})	0.14 ± 0.06 ($p \leq 0.05$)	0.07 ± 0.05 ($p = 0.16$)

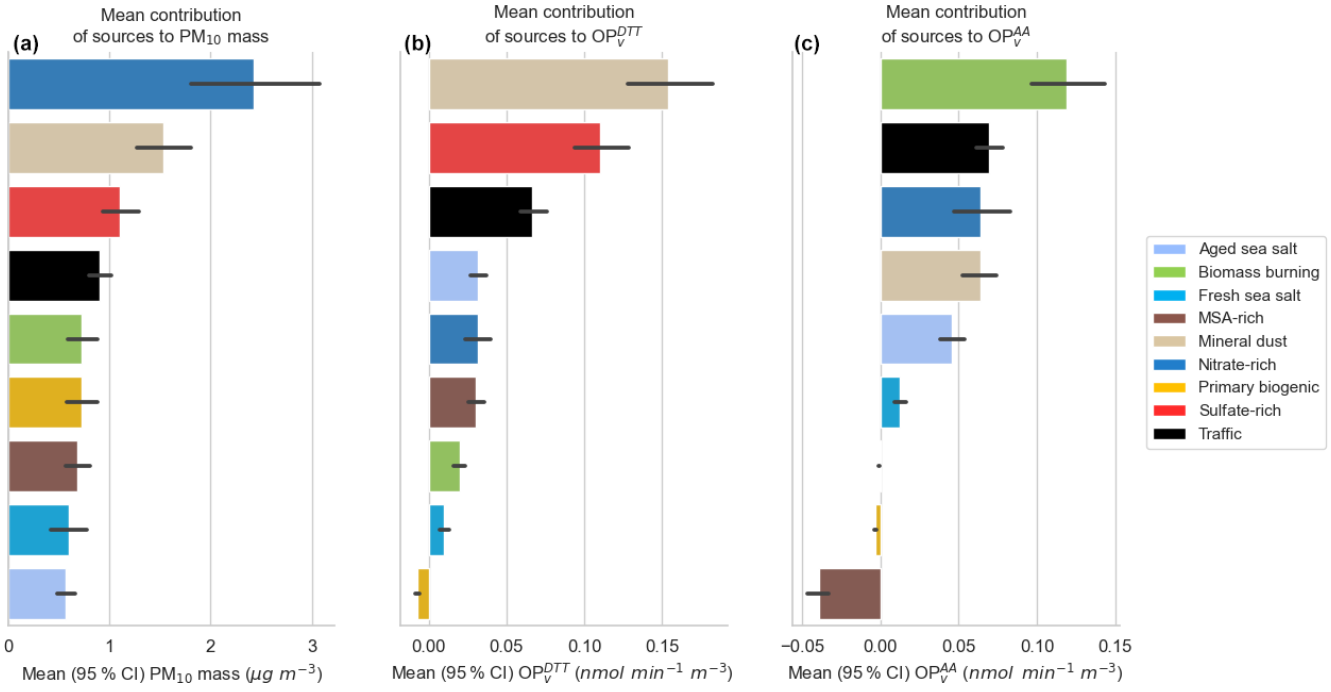

Figure 10. Overall daily mean OP_v contribution of the sources to PM_{10} and OP activity (OP_v^{DTT} and OP_v^{AA}) using MLR analysis in the form of mean and 95 % confidence interval of the mean (error bar) ($n = 168$ samples).

ber et al., 2021). With the use of fit-for-purpose organic tracers, possible mixing issues in these factors can be minimized (Borlaza et al., 2021a). However, these supplementary tracers were not available at the OPE site, making it difficult to eliminate potential influence from other factors or species in PM.

Figure 12 presents the yearly contribution of each factor to the OP of PM_{10} for the 3 years investigated in this study. There is no clear decreasing trend in the total OP reconstructed by MLR analysis. Although there is a decreasing trend found in the mass contributions of the traffic factor, this was not clearly reflected in its OP contributions. The other sources seem to have comparatively consistent OP contributions from 2017 to 2020, and no notable tendency can be found in the total OP contribution as opposed to the contributions to PM_{10} mass showing decreasing trends. This may be explained by the limited subset of samples for the OP assay (OP data spanning 4 years against 9 years for the PMF data), the shorter time range being insufficient to reach significance and robustness in the trend assessment of OP levels.

3.8 Limitations of the study

In spite of the advantages offered by the long-term monitoring at the OPE site, there were a few limitations encountered

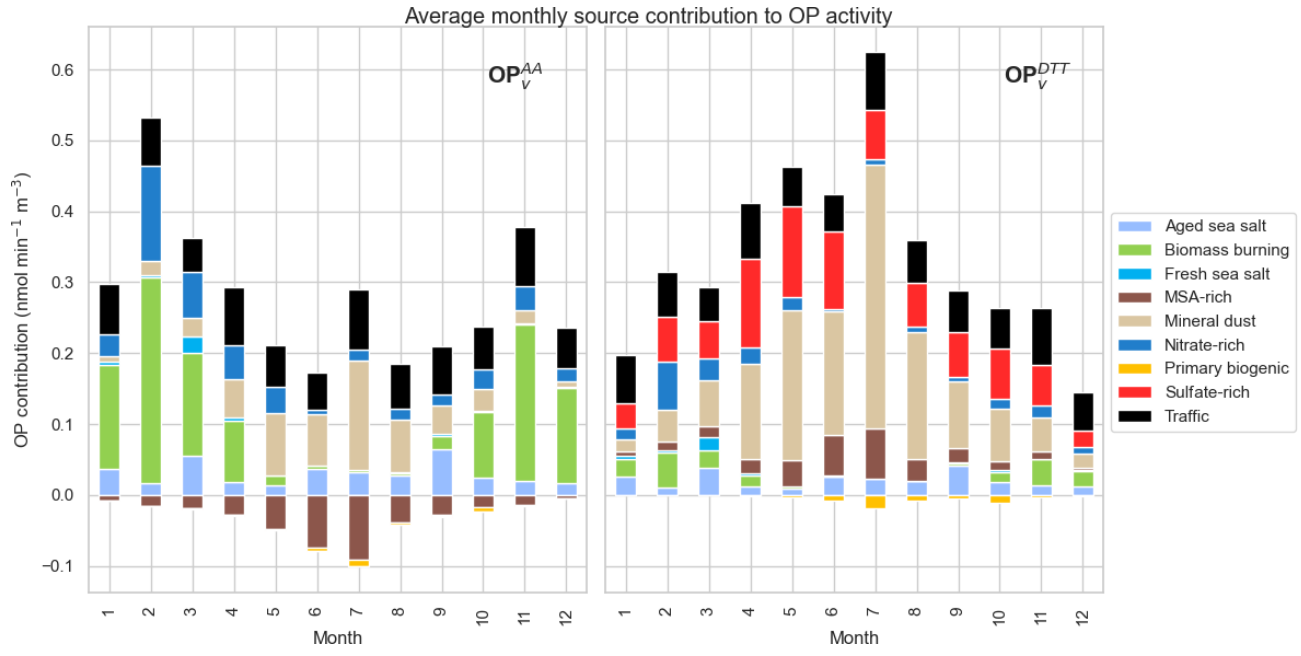

Figure 11. Monthly contribution of sources to OP activity in nmol min^{-1} m^{-3} (OP_v^{DTT} and OP_v^{AA}) from the year 2017 to 2020 at the OPE site. Note that the months are labelled from January (1) to December (12).

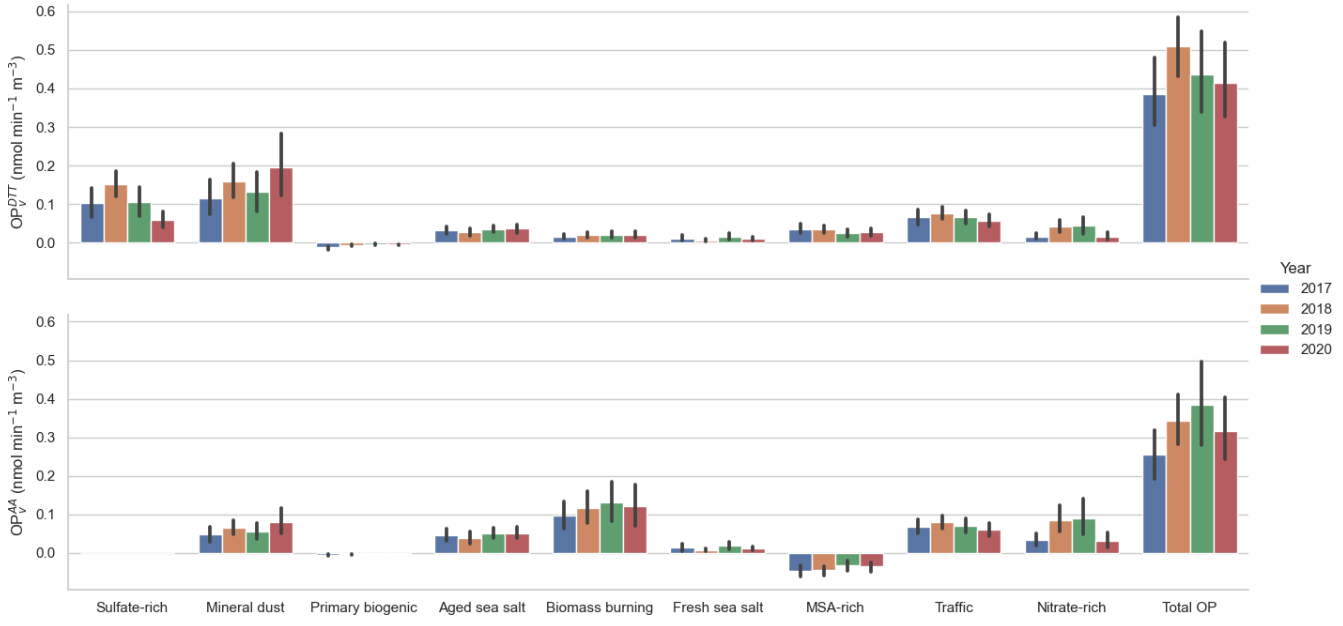

Figure 12. Yearly average contributions of sources to OP activity in nmol min^{-1} m^{-3} (OP_v^{DTT} and OP_v^{AA}) from the year 2017 to 2020 at the OPE site. Note that total OP is the sum of OP contributions of all sources as modelled by the MLR analysis.

during the investigation of the dataset. Each limitation is discussed as follows:

- There was a change in sampling duration between the collection performed in year 2012 to 2016 (7 d sampling) and 2016 to 2020 (24 h sampling). A 7 d filter sample includes both weekdays and weekends, whereas a 24 h sample will either be a weekday or weekend, depending on the sampling interval. This implies that the weekly collected samples may contain particles that are not fully captured in a daily sample. However, since the OPE site is quite distant from direct emissions, the expected difference in the weekday and weekend levels should be relatively small. Further, PMF source ap-

portionment was conducted separately (i.e. 7 d samples versus 24 h samples), leading to very similar results for the chemical profiles and source contributions, justifying the coupled analysis (see Supplement, Table S4 and Figs. S13 to S21).

- There is a lack of fit-for-purpose tracers to fully elucidate the influence of SOA in a site with relevant distance from direct emissions (or rural typology) such as OPE. In Borlaza et al. (2021a), a secondary biogenic oxidation source was additionally identified using organic tracers (3-MBTCA and pinic acid), while anthropogenic influence was supported by contributions of phthalic acid, even in secondary aerosol sources. With the typology at the OPE site, this would have been useful.

- The use of a single chemical profile for long-term PM source apportionment could be limiting for the PMF model. As we have found consistent decrease in some species, particularly EC, perhaps a rolling PMF (e.g. yearly PMF) could better capture possible changes in the source profiles.

- The absence of samples for OP analysis from the years prior to 2017 has limited the investigation of long-term OP at the OPE site. Consequently, it was not easy to capture the decrease in OP contributions from the traffic factor as similarly captured in the mass contributions. Perhaps a hindcasting method on the years without OP data could have been performed; however that would heavily rely on the OP_m modelled from the year 2017 to 2020, which can lead to bias in the results.

- In the year 2020, a series of lockdown restrictions were placed nationally as a response to the coronavirus disease (COVID-19) pandemic. In the OPE site, there is no clear decrease in average PM_{10} mass concentration in 2020 (Fig. 12) that could have greatly affected the results of this study. In fact, excluding all samples from the year 2020, the traffic factor contributions to PM_{10} still has a reduction of 39 % from the year 2012 to 2019 and an overall yearly average reduction of 135 ng m^{-3} yr^{-1} ($p \leq 0.01$).

4 Conclusions

Over the 9-year analysis in a rural background site in France (OPE), the observed PM_{10} mass concentration and OP were found to be much lower than other sites in France. The sources of PM_{10} mass and OP were apportioned using PMF and MLR analysis, respectively. The nine identified factors relevant for PM_{10} include secondary inorganics (nitrate- and sulfate-rich), traffic, mineral dust, biomass burning, sea salts (fresh and aged), primary biogenic, and MSA-rich.

A redistribution of the factor impacts between mass and OP contributions was observed, underlining the importance of taking into account the redox activity of PM when considering their potential health effects. Based on PM mass, the major contributors are nitrate- and sulfate-rich factors, both factors being associated with secondary inorganics formed during long range transport (LRT). On the other hand, based on OP activity, the main contributors are mostly anthropogenic-derived sources such as traffic, mineral dust, and biomass burning factors.

As the OPE site is located far from direct anthropogenic emissions, the influence of LRT processes was noted in some sources. Sources such as sulfate- and nitrate-rich, MSA-rich, and aged sea salt factors have shown potential mixing with other anthropogenic sources, most probably due to the transit time. These potential mixing and ageing processes were reflected in the chemical mass profile of each factor as well as in their OP contributions.

Thanks to the long-term dataset at the OPE site, it was observed that the traffic factor contribution to total PM_{10} has decreased over the years for this site that may well represent the French national background PM. This decrease is much larger than any change observed for the other PM sources and is in excellent agreement with estimations in the decrease in BC emissions from the transport sector all over France from the national inventory. This effect may be attributed to improvement of the exhaust emission of terrestrial transportation fleet, and/or to regulations restricting vehicular emissions in bigger cities and/or other regional-scale. However, persistent changes in meteorological conditions influencing the transport of air masses to OPE or formation of PM during this transport cannot be totally ruled out.

Code availability. The software code can be made available upon request by contacting the corresponding author.

Data availability. The chemical, PMF, and OP datasets can be made available upon request by contacting the corresponding author. The data used for the comparison in Fig. 8 are obtained from many different programmes, including the CARA programme coordinated by Olivier Favez (Favez et al., 2021).

Supplement. The supplement related to this article is available online at: https://doi.org/10.5194/acp-22-8701-2022-supplement.

Author contributions. SC manages the overall observatory at OPE, including the supervision of the PM sampling. JLJ designed the project, in collaboration with SC. LJB, SW, and AM did the curation of the database. LJB performed the data analysis and wrote the paper. GU managed the OP analytical procedures at IGE. VJ designed part of the analytical method on the Air O Sol plateau. MC is the representation of Atmo GE, who helped maintain the sampling equipment. JLB was in charge of the coordination of different

research programs and funding acquisitions. All authors read and commented on the paper.

Competing interests. The contact author has declared that none of the authors has any competing interests.

Disclaimer. Publisher's note: Copernicus Publications remains neutral with regard to jurisdictional claims in published maps and institutional affiliations.

Acknowledgements. The authors wish to thank all the many people from the different laboratories (OPE, IGE, Air O Sol analytical platform, LCME) and from the regional air quality monitoring network Atmos Grand Est, who have actively contributed to filter sampling and/or analysis over the years.

Review statement. This paper was edited by Leiming Zhang and reviewed by three anonymous referees.

References

Aas, W., Tsyro, S., Bieber, E., Bergström, R., Ceburnis, D., Ellermann, T., Fagerli, H., Frölich, M., Gehrig, R., Makkonen, U., Nemitz, E., Otjes, R., Perez, N., Perrino, C., Prévôt, A. S. H., Putaud, J.-P., Simpson, D., Spindler, G., Vana, M., and Yttri, K. E.: Lessons learnt from the first EMEP intensive measurement periods, Atmos. Chem. Phys., 12, 8073–8094, https://doi.org/10.5194/acp-12-8073-2012, 2012.

Alastuey, A., Querol, X., Aas, W., Lucarelli, F., Pérez, N., Moreno, T., Cavalli, F., Areskoug, H., Balan, V., Catrambone, M., Ceburnis, D., Cerro, J. C., Conil, S., Gevorgyan, L., Hueglin, C., Imre, K., Jaffrezo, J.-L., Leeson, S. R., Mihalopoulos, N., Mitosinkova, M., O'Dowd, C. D., Pey, J., Putaud, J.-P., Riffault, V., Ripoll, A., Sciare, J., Sellegri, K., Spindler, G., and Yttri, K. E.: Geochemistry of PM_{10} over Europe during the EMEP intensive measurement periods in summer 2012 and winter 2013, Atmos. Chem. Phys., 16, 6107–6129, https://doi.org/10.5194/acp-16-6107-2016, 2016.

Alleman, L. Y., Lamaison, L., Perdrix, E., Robache, A., and Galloo, J.-C.: PM_{10} metal concentrations and source identification using positive matrix factorization and wind sectoring in a French industrial zone, Atmos. Res., 96, 612–625, https://doi.org/10.1016/j.atmosres.2010.02.008, 2010.

Amato, F., Alastuey, A., de la Rosa, J., Gonzalez Castanedo, Y., Sánchez de la Campa, A. M., Pandolfi, M., Lozano, A., Contreras González, J., and Querol, X.: Trends of road dust emissions contributions on ambient air particulate levels at rural, urban and industrial sites in southern Spain, Atmos. Chem. Phys., 14, 3533–3544, https://doi.org/10.5194/acp-14-3533-2014, 2014.

Anenberg, S. C., Horowitz, L. W., Tong, D. Q., and West, J. J.: An Estimate of the Global Burden of Anthropogenic Ozone and Fine Particulate Matter on Premature Human Mortality Using Atmospheric Modeling, Environ. Health Persp., 118, 1189–1195, https://doi.org/10.1289/ehp.0901220, 2010.

Barmpadimos, I., Keller, J., Oderbolz, D., Hueglin, C., and Prévôt, A. S. H.: One decade of parallel fine ($PM_{2.5}$) and coarse (PM_{10}–$PM_{2.5}$) particulate matter measurements in Europe: trends and variability, Atmos. Chem. Phys., 12, 3189–3203, https://doi.org/10.5194/acp-12-3189-2012, 2012.

Barrie, L. A. and Hoff, R. M.: Five years of air chemistry observations in the Canadian Arctic, Atmos. Environ., 19, 1995–2010, https://doi.org/10.1016/0004-6981(85)90108-8, 1985.

Bates, J. T., Fang, T., Verma, V., Zeng, L., Weber, R. J., Tolbert, P. E., Abrams, J. Y., Sarnat, S. E., Klein, M., Mulholland, J. A., and Russell, A. G.: Review of Acellular Assays of Ambient Particulate Matter Oxidative Potential: Methods and Relationships with Composition, Sources, and Health Effects, Environ. Sci. Technol., 53, 4003–4019, https://doi.org/10.1021/acs.est.8b03430, 2019.

Belis, C. A.: European guide on air pollution source apportionment with receptor models: revised version 2019, Publications Office, LU, ISBN 9276090010, 2019.

Belis, C. A., Pernigotti, D., Karagulian, F., Pirovano, G., Larsen, B. R., Gerboles, M., and Hopke, P. K.: A new methodology to assess the performance and uncertainty of source apportionment models in intercomparison exercises, Atmos. Environ., 119, 35–44, https://doi.org/10.1016/j.atmosenv.2015.08.002, 2015.

Bernard, Y., Miller, J., Wappelhorst, S., and Braun, C.: Impacts of the Paris Low-Emission Zone and Implications for Other Cities, TRUE – The Real Urban Emissions Initiative, United Kingdom, ISBN 01744072, 2020.

Bessagnet, B., Menut, L., Lapere, R., Couvidat, F., Jaffrezo, J.-L., Mailler, S., Favez, O., Pennel, R., and Siour, G.: High Resolution Chemistry Transport Modeling with the On-Line CHIMERE-WRF Model over the French Alps – Analysis of a Feedback of Surface Particulate Matter Concentrations on Mountain Meteorology, Atmosphere, 11, 565, https://doi.org/10.3390/atmos11060565, 2020.

Birch, M. E. and Cary, R. A.: Elemental Carbon-Based Method for Monitoring Occupational Exposures to Particulate Diesel Exhaust, Aerosol Sci. Tech., 25, 221–241, https://doi.org/10.1080/02786829608965393, 1996.

Borlaza, L. J. S., Weber, S., Uzu, G., Jacob, V., Cañete, T., Micallef, S., Trébuchon, C., Slama, R., Favez, O., and Jaffrezo, J.-L.: Disparities in particulate matter (PM_{10}) origins and oxidative potential at a city scale (Grenoble, France) – Part 1: Source apportionment at three neighbouring sites, Atmos. Chem. Phys., 21, 5415–5437, https://doi.org/10.5194/acp-21-5415-2021, 2021a.

Borlaza, L. J. S., Weber, S., Jaffrezo, J.-L., Houdier, S., Slama, R., Rieux, C., Albinet, A., Micallef, S., Trébluchon, C., and Uzu, G.: Disparities in particulate matter (PM_{10}) origins and oxidative potential at a city scale (Grenoble, France) – Part 2: Sources of PM_{10} oxidative potential using multiple linear regression analysis and the predictive applicability of multilayer perceptron neural network analysis, Atmos. Chem. Phys., 21, 9719–9739, https://doi.org/10.5194/acp-21-9719-2021, 2021b.

Bozzetti, C., El Haddad, I., Salameh, D., Daellenbach, K. R., Fermo, P., Gonzalez, R., Minguillón, M. C., Iinuma, Y., Poulain, L., Elser, M., Müller, E., Slowik, J. G., Jaffrezo, J.-L., Baltensperger, U., Marchand, N., and Prévôt, A. S. H.: Organic aerosol source apportionment by offline-AMS over a full year in Marseille, Atmos. Chem. Phys., 17, 8247–8268, https://doi.org/10.5194/acp-17-8247-2017, 2017.

Brattich, E., Orza, J. A. G., Cristofanelli, P., Bonasoni, P., Marinoni, A., and Tositti, L.: Advection pathways at the Mt. Cimone WMO-GAW station: Seasonality, trends, and influence on atmospheric composition, Atmos. Environ., 234, 117513, https://doi.org/10.1016/j.atmosenv.2020.117513, 2020.

Brighty, A., Jacob, V., Uzu, G., Borlaza, L., Conil, S., Hueglin, C., Grange, S. K., Favez, O., Trébuchon, C., and Jaffrezo, J.-L.: Cellulose in atmospheric particulate matter at rural and urban sites across France and Switzerland, Atmos. Chem. Phys., 22, 6021–6043, https://doi.org/10.5194/acp-22-6021-2022, 2022.

Calas, A., Uzu, G., Martins, J. M. F., Voisin, D., Spadini, L., Lacroix, T., and Jaffrezo, J.-L.: The importance of simulated lung fluid (SLF) extractions for a more relevant evaluation of the oxidative potential of particulate matter, Sci. Rep., 7, 11617, https://doi.org/10.1038/s41598-017-11979-3, 2017.

Calas, A., Uzu, G., Kelly, F. J., Houdier, S., Martins, J. M. F., Thomas, F., Molton, F., Charron, A., Dunster, C., Oliete, A., Jacob, V., Besombes, J.-L., Chevrier, F., and Jaffrezo, J.-L.: Comparison between five acellular oxidative potential measurement assays performed with detailed chemistry on PM_{10} samples from the city of Chamonix (France), Atmos. Chem. Phys., 18, 7863–7875, https://doi.org/10.5194/acp-18-7863-2018, 2018.

Calas, A., Uzu, G., Besombes, J.-L., Martins, J. M. F., Redaelli, M., Weber, S., Charron, A., Albinet, A., Chevrier, F., Brulfert, G., Mesbah, B., Favez, O., and Jaffrezo, J.-L.: Seasonal Variations and Chemical Predictors of Oxidative Potential (OP) of Particulate Matter (PM), for Seven Urban French Sites, Atmosphere, 10, 698, https://doi.org/10.3390/atmos10110698, 2019.

Canonaco, F., Tobler, A., Chen, G., Sosedova, Y., Slowik, J. G., Bozzetti, C., Daellenbach, K. R., El Haddad, I., Crippa, M., Huang, R.-J., Furger, M., Baltensperger, U., and Prévôt, A. S. H.: A new method for long-term source apportionment with time-dependent factor profiles and uncertainty assessment using SoFi Pro: application to 1 year of organic aerosol data, Atmos. Meas. Tech., 14, 923–943, https://doi.org/10.5194/amt-14-923-2021, 2021.

Cassee, F. R., Héroux, M.-E., Gerlofs-Nijland, M. E., and Kelly, F. J.: Particulate matter beyond mass: recent health evidence on the role of fractions, chemical constituents and sources of emission, Inhal. Toxicol., 25, 802–812, https://doi.org/10.3109/08958378.2013.850127, 2013.

Cesari, D., Merico, E., Grasso, F. M., Decesari, S., Belosi, F., Manarini, F., De Nuntiis, P., Rinaldi, M., Volpi, F., Gambaro, A., Morabito, E., and Contini, D.: Source Apportionment of $PM_{2.5}$ and of its Oxidative Potential in an Industrial Suburban Site in South Italy, Atmosphere, 10, 758, https://doi.org/10.3390/atmos10120758, 2019.

Charrier, J. G. and Anastasio, C.: On dithiothreitol (DTT) as a measure of oxidative potential for ambient particles: evidence for the importance of soluble transition metals, Atmos. Chem. Phys., 12, 9321–9333, https://doi.org/10.5194/acp-12-9321-2012, 2012.

Charrier, J. G., McFall, A. S., Richards-Henderson, N. K., and Anastasio, C.: Hydrogen Peroxide Formation in a Surrogate Lung Fluid by Transition Metals and Quinones Present in Particulate Matter, Environ. Sci. Technol., 48, 7010–7017, https://doi.org/10.1021/es501011w, 2014.

Charron, A., Polo-Rehn, L., Besombes, J.-L., Golly, B., Buisson, C., Chanut, H., Marchand, N., Guillaud, G., and Jaffrezo, J.-L.: Identification and quantification of particulate tracers of exhaust and non-exhaust vehicle emissions, Atmos. Chem. Phys., 19, 5187–5207, https://doi.org/10.5194/acp-19-5187-2019, 2019.

Chen, Q., Sherwen, T., Evans, M., and Alexander, B.: DMS oxidation and sulfur aerosol formation in the marine troposphere: a focus on reactive halogen and multiphase chemistry, Atmos. Chem. Phys., 18, 13617–13637, https://doi.org/10.5194/acp-18-13617-2018, 2018.

Chen, Z., Chen, D., Zhao, C., Kwan, M., Cai, J., Zhuang, Y., Zhao, B., Wang, X., Chen, B., Yang, J., Li, R., He, B., Gao, B., Wang, K., and Xu, B.: Influence of meteorological conditions on $PM_{2.5}$ concentrations across China: A review of methodology and mechanism, Environ. Int., 139, 105558, https://doi.org/10.1016/j.envint.2020.105558, 2020.

Cho, A. K., Sioutas, C., Miguel, A. H., Kumagai, Y., Schmitz, D. A., Singh, M., Eiguren-Fernandez, A., and Froines, J. R.: Redox activity of airborne particulate matter at different sites in the Los Angeles Basin, Environ. Res., 99, 40–47, https://doi.org/10.1016/j.envres.2005.01.003, 2005.

Cleveland, R., Cleveland, W., McRae, J., and Terpenning, I.: STL: A seasonal-trend decomposition procedure based on LOESS, J. Off. Stat., 6, 3–73, 1990.

Conil, S., Helle, J., Langrene, L., Laurent, O., Delmotte, M., and Ramonet, M.: Continuous atmospheric CO_2, CH_4 and CO measurements at the Observatoire Pérenne de l'Environnement (OPE) station in France from 2011 to 2018, Atmos. Meas. Tech., 12, 6361–6383, https://doi.org/10.5194/amt-12-6361-2019, 2019.

Conte, E., Canepari, S., Frasca, D., and Simonetti, G.: Oxidative Potential of Selected PM Components, Proceedings, 1, 108, https://doi.org/10.3390/ecas2017-04131, 2017.

Crobeddu, B., Aragao-Santiago, L., Bui, L.-C., Boland, S., and Baeza Squiban, A.: Oxidative potential of particulate matter 2.5 as predictive indicator of cellular stress, Environm. Pollut., 230, 125–133, https://doi.org/10.1016/j.envpol.2017.06.051, 2017.

Cusack, M., Alastuey, A., Pérez, N., Pey, J., and Querol, X.: Trends of particulate matter ($PM_{2.5}$) and chemical composition at a regional background site in the Western Mediterranean over the last nine years (2002–2010), Atmos. Chem. Phys., 12, 8341–8357, https://doi.org/10.5194/acp-12-8341-2012, 2012.

Czernecki, B., Półrolniczak, M., Kolendowicz, L., Marosz, M., Kendzierski, S., and Pilguj, N.: Influence of the atmospheric conditions on PM_{10} concentrations in Poznań, Poland, J. Atmos. Chem., 74, 115–139, https://doi.org/10.1007/s10874-016-9345-5, 2017.

Daellenbach, K. R., Uzu, G., Jiang, J., Cassagnes, L.-E., Leni, Z., Vlachou, A., Stefenelli, G., Canonaco, F., Weber, S., Segers, A., Kuenen, J. J. P., Schaap, M., Favez, O., Albinet, A., Aksoyoglu, S., Dommen, J., Baltensperger, U., Geiser, M., El Haddad, I., Jaffrezo, J.-L., and Prévôt, A. S. H.: Sources of particulate-matter air pollution and its oxidative potential in Europe, Nature, 587, 414–419, https://doi.org/10.1038/s41586-020-2902-8, 2020.

Dou, J., Lin, P., Kuang, B.-Y., and Yu, J. Z.: Reactive Oxygen Species Production Mediated by Humic-like Substances in Atmospheric Aerosols: Enhancement Effects by Pyridine, Imidazole, and Their Derivatives, Environ. Sci. Technol., 49, 6457–6465, https://doi.org/10.1021/es5059378, 2015.

Fang, T., Guo, H., Zeng, L., Verma, V., Nenes, A., and Weber, R. J.: Highly Acidic Ambient Particles, Soluble Metals, and Oxidative Potential: A Link between Sulfate and

Aerosol Toxicity, Environ. Sci. Technol., 51, 2611–2620, https://doi.org/10.1021/acs.est.6b06151, 2017.

Favez, O., El Haddad, I., Piot, C., Boréave, A., Abidi, E., Marchand, N., Jaffrezo, J.-L., Besombes, J.-L., Personnaz, M.-B., Sciare, J., Wortham, H., George, C., and D'Anna, B.: Inter-comparison of source apportionment models for the estimation of wood burning aerosols during wintertime in an Alpine city (Grenoble, France), Atmos. Chem. Phys., 10, 5295–5314, https://doi.org/10.5194/acp-10-5295-2010, 2010.

Favez, O., Weber, S., Petit, J.-E., Alleman, L. Y., Albinet, A., Riffault, V., Chazeau, B., Amodeo, T., Salameh, D., Zhang, Y., Srivastava, D., Samaké, A., Aujay-Plouzeau, R., Papin, A., Bonnaire, N., Boullanger, C., Chatain, M., Chevrier, F., Detournay, A., Dominik-Sègue, M., Falhun, R., Garbin, C., Ghersi, V., Grignion, G., Levigoureux, G., Pontet, S., Rangognio, J., Zhang, S., Besombes, J.-L., Conil, S., Uzu, G., Savarino, J., Marchand, N., Gros, V., Marchand, C., Jaffrezo, J.-L., and Leoz-Garziandia, E.: Overview of the French Operational Network for In Situ Observation of PM Chemical Composition and Sources in Urban Environments (CARA Program), Atmosphere, 12, 207, https://doi.org/10.3390/atmos12020207, 2021.

Gama, C., Monteiro, A., Pio, C., Miranda, A. I., Baldasano, J. M., and Tchepel, O.: Temporal patterns and trends of particulate matter over Portugal: a long-term analysis of background concentrations, Air Qual. Atmos. Health, 11, 397–407, https://doi.org/10.1007/s11869-018-0546-8, 2018.

Gao, D., Ripley, S., Weichenthal, S., and Godri Pollitt, K. J.: Ambient particulate matter oxidative potential: Chemical determinants, associated health effects, and strategies for risk management, Free Radical Biol. Med., 151, 7–25, https://doi.org/10.1016/j.freeradbiomed.2020.04.028, 2020a.

Gao, D., Mulholland, J. A., Russell, A. G., and Weber, R. J.: Characterization of water-insoluble oxidative potential of $PM_{2.5}$ using the dithiothreitol assay, Atmos. Environ., 224, 117327, https://doi.org/10.1016/j.atmosenv.2020.117327, 2020b.

Gianini, M. F. D., Fischer, A., Gehrig, R., Ulrich, A., Wichser, A., Piot, C., Besombes, J.-L., and Hueglin, C.: Comparative source apportionment of PM_{10} in Switzerland for 2008/2009 and 1998/1999 by Positive Matrix Factorisation, Atmos. Environ., 54, 149–158, https://doi.org/10.1016/j.atmosenv.2012.02.036, 2012.

Golly, B., Waked, A., Weber, S., Samake, A., Jacob, V., Conil, S., Rangognio, J., Chrétien, E., Vagnot, M.-P., Robic, P.-Y., Besombes, J.-L., and Jaffrezo, J.-L.: Organic markers and OC source apportionment for seasonal variations of $PM_{2.5}$ at 5 rural sites in France, Atmos. Environ., 198, 142–157, https://doi.org/10.1016/j.atmosenv.2018.10.027, 2019.

Grange, S. K., Fischer, A., Zellweger, C., Alastuey, A., Querol, X., Jaffrezo, J.-L., Weber, S., Uzu, G., and Hueglin, C.: Switzerland's PM_{10} and $PM_{2.5}$ environmental increments show the importance of non-exhaust emissions, Atmos. Environ., 12, 100145, https://doi.org/10.1016/j.aeaoa.2021.100145, 2021.

Guascito, M. R., Pietrogrande, M. C., Decesari, S., and Contini, D.: Oxidative Potential of Atmospheric Aerosols, Atmosphere, 12, 531, https://doi.org/10.3390/atmos12050531, 2021.

Hand, J. L., Schichtel, B. A., Pitchford, M., Malm, W. C., and Frank, N. H.: Seasonal composition of remote and urban fine particulate matter in the United States, 117, D05209, https://doi.org/10.1029/2011JD017122, 2012.

Handler, M., Puls, C., Zbiral, J., Marr, I., Puxbaum, H., and Limbeck, A.: Size and composition of particulate emissions from motor vehicles in the Kaisermühlen-Tunnel, Vienna, Atmos. Environ., 42, 2173–2186, https://doi.org/10.1016/j.atmosenv.2007.11.054, 2008.

Henderson, P. and Henderson, G.: The Cambridge handbook of earth science data, Choice Reviews Online, 47, 2354, https://doi.org/10.5860/CHOICE.47-2354, 2010.

Herich, H., Gianini, M. F. D., Piot, C., Močnik, G., Jaffrezo, J.-L., Besombes, J.-L., Prévôt, A. S. H., and Hueglin, C.: Overview of the impact of wood burning emissions on carbonaceous aerosols and PM in large parts of the Alpine region, Atmos. Environ., 89, 64–75, https://doi.org/10.1016/j.atmosenv.2014.02.008, 2014.

Hou, P. and Wu, S.: Long-term Changes in Extreme Air Pollution Meteorology and the Implications for Air Quality, Sci. Rep., 6, 23792, https://doi.org/10.1038/srep23792, 2016.

Jaffrezo, J.-L., Davidson, C. I., Kuhns, H. D., Bergin, M. H., Hillamo, R., Maenhaut, W., Kahl, J. W., and Harris, J. M.: Biomass burning signatures in the atmosphere of central Greenland, J. Geophys. Res., 103, 31067–31078, https://doi.org/10.1029/98JD02241, 1998.

Jardine, K., Yañez-Serrano, A. M., Williams, J., Kunert, N., Jardine, A., Taylor, T., Abrell, L., Artaxo, P., Guenther, A., Hewitt, C. N., House, E., Florentino, A. P., Manzi, A., Higuchi, N., Kesselmeier, J., Behrendt, T., Veres, P. R., Derstroff, B., Fuentes, J. D., Martin, S. T., and Andreae, M. O.: Dimethyl sulfide in the Amazon rain forest: DMS in the Amazon, Global Biogeochem. Cy., 29, 19–32, https://doi.org/10.1002/2014GB004969, 2015.

Jiang, H., Ahmed, C. M. S., Canchola, A., Chen, J. Y., and Lin, Y. H.: Use of Dithiothreitol Assay to Evaluate the Oxidative Potential of Atmospheric Aerosols, Atmosphere, 10, 571, https://doi.org/10.3390/atmos10100571, 2019.

Johnson, D., Utembe, S. R., Jenkin, M. E., Derwent, R. G., Hayman, G. D., Alfarra, M. R., Coe, H., and McFiggans, G.: Simulating regional scale secondary organic aerosol formation during the TORCH 2003 campaign in the southern UK, Atmos. Chem. Phys., 6, 403–418, https://doi.org/10.5194/acp-6-403-2006, 2006.

Kelly, F. J. and Mudway, I. S.: Protein oxidation at the air-lung interface, Amino Acids, 25, 375–396, https://doi.org/10.1007/s00726-003-0024-x, 2003.

Kim, M. J.: Changes in the Relationship between Particulate Matter and Surface Temperature in Seoul from 2002–2017, Atmosphere, 10, 238, https://doi.org/10.3390/atmos10050238, 2019.

Konovalov, I. B., Beekmann, M., Meleux, F., Dutot, A., and Foret, G.: Combining deterministic and statistical approaches for PM_{10} forecasting in Europe, Atmos. Environ., 43, 6425–6434, https://doi.org/10.1016/j.atmosenv.2009.06.039, 2009.

Li, J., Chen, B., de la Campa, A. M. S., Alastuey, A., Querol, X., and de la Rosa, J. D.: 2005–2014 trends of PM_{10} source contributions in an industrialized area of southern Spain, Environm. Pollut., 236, 570–579, https://doi.org/10.1016/j.envpol.2018.01.101, 2018.

Li, S.-M., Barrie, L. A., Talbot, R. W., Harriss, R. C., Davidson, C. I., and Jaffrezo, J.-L.: Seasonal and geographic variations of methanesulfonic acid in the arctic troposphere, Atmos. Environ. A-Gen., 27, 3011–3024, https://doi.org/10.1016/0960-1686(93)90333-T, 1993.

Miyazaki, Y., Fu, P. Q., Kawamura, K., Mizoguchi, Y., and Yamanoi, K.: Seasonal variations of stable carbon isotopic composition and biogenic tracer compounds of water-soluble organic aerosols in a deciduous forest, Atmos. Chem. Phys., 12, 1367–1376, https://doi.org/10.5194/acp-12-1367-2012, 2012.

Møller, P., Jacobsen, N. R., Folkmann, J. K., Danielsen, P. H., Mikkelsen, L., Hemmingsen, J. G., Vesterdal, L. K., Forchhammer, L., Wallin, H., and Loft, S.: Role of oxidative damage in toxicity of particulates, Free Radical Res., 44, 1–46, https://doi.org/10.3109/10715760903300691, 2010.

Moroni, B., Cappelletti, D., Ferrero, L., Crocchianti, S., Busetto, M., Mazzola, M., Becagli, S., Traversi, R., and Udisti, R.: Local vs. long-range sources of aerosol particles upon Ny-Ålesund (Svalbard Islands): mineral chemistry and geochemical records, Rend. Fis. Acc. Lincei, 27, 115–127, https://doi.org/10.1007/s12210-016-0533-7, 2016.

Mues, A., Manders, A., Schaap, M., van Ulft, L. H., van Meijgaard, E., and Builtjes, P.: Differences in particulate matter concentrations between urban and rural regions under current and changing climate conditions, Atmos. Environ., 80, 232–247, https://doi.org/10.1016/j.atmosenv.2013.07.049, 2013.

Nejedlý, Z., Campbell, J. L., Teesdale, W. J., Dlouhy, J. F., Dann, T. F., Hoff, R. M., Brook, J. R., and Wiebe, H. A.: Inter-Laboratory Comparison of Air Particulate Monitoring Data, J. Air Waste Manage. Assoc., 48, 386–397, https://doi.org/10.1080/10473289.1998.10463698, 1998.

Nel, A.: ATMOSPHERE: Enhanced: Air Pollution-Related Illness: Effects of Particles, Science, 308, 804–806, https://doi.org/10.1126/science.1108752, 2005.

Norris, G., Duvall, R., Brown, S., and Bai, S.: Positive Matrix Factorization (PMF) 5.0 Fundamentals and User Guide, 136, Record ID: 308292, 2014.

Oh, S.-H., Song, M., Schauer, J. J., Shon, Z.-H., and Bae, M.-S.: Assessment of long-range oriented source and oxidative potential on the South-west shoreline, Korea: Molecular marker receptor models during shipborne measurements, Environm. Pollut., 281, 116979, https://doi.org/10.1016/j.envpol.2021.116979, 2021.

Paatero, P. and Tapper, U.: Positive matrix factorization: A non-negative factor model with optimal utilization of error estimates of data values, Environmetrics, 5, 111–126, https://doi.org/10.1002/env.3170050203, 1994.

Pandolfi, M., Alastuey, A., Pérez, N., Reche, C., Castro, I., Shatalov, V., and Querol, X.: Trends analysis of PM source contributions and chemical tracers in NE Spain during 2004–2014: a multiexponential approach, Atmos. Chem. Phys., 16, 11787–11805, https://doi.org/10.5194/acp-16-11787-2016, 2016.

Pappalardo, G.: ACTRIS Aerosol, Clouds and Trace Gases Research Infrastructure, EPJ Web Conf., 176, 09004, https://doi.org/10.1051/epjconf/201817609004, 2018.

Paraskevopoulou, D., Bougiatioti, A., Stavroulas, I., Fang, T., Lianou, M., Liakakou, E., Gerasopoulos, E., Weber, R., Nenes, A., and Mihalopoulos, N.: Yearlong variability of oxidative potential of particulate matter in an urban Mediterranean environment, Atmos. Environ., 206, 183–196, https://doi.org/10.1016/j.atmosenv.2019.02.027, 2019.

Park, M., Joo, H. S., Lee, K., Jang, M., Kim, S. D., Kim, I., Borlaza, L. J. S., Lim, H., Shin, H., Chung, K. H., Choi, Y.-H., Park, S. G., Bae, M.-S., Lee, J., Song, H., and Park, K.: Differential toxicities of fine particulate matters from various sources, Sci. Rep., 8, 17007, https://doi.org/10.1038/s41598-018-35398-0, 2018.

Pernigotti, D. and Belis, C. A.: DeltaSA tool for source apportionment benchmarking, description and sensitivity analysis, Atmos. Environ., 180, 138–148, https://doi.org/10.1016/j.atmosenv.2018.02.046, 2018.

Pey, J., Pérez, N., Castillo, S., Viana, M., Moreno, T., Pandolfi, M., López-Sebastián, J. M., Alastuey, A., and Querol, X.: Geochemistry of regional background aerosols in the Western Mediterranean, Atmos. Res., 94, 422–435, https://doi.org/10.1016/j.atmosres.2009.07.001, 2009.

Pietrogrande, M. C., Russo, M., and Zagatti, E.: Review of PM Oxidative Potential Measured with Acellular Assays in Urban and Rural Sites across Italy, Atmosphere, 10, 626, https://doi.org/10.3390/atmos10100626, 2019.

Pio, C., Cerqueira, M., Harrison, R. M., Nunes, T., Mirante, F., Alves, C., Oliveira, C., Sanchez de la Campa, A., Artíñano, B., and Matos, M.: OC / EC ratio observations in Europe: Rethinking the approach for apportionment between primary and secondary organic carbon, Atmos. Environ., 45, 6121–6132, https://doi.org/10.1016/j.atmosenv.2011.08.045, 2011.

Putaud, J.-P., Raes, F., Van Dingenen, R., Brüggemann, E., Facchini, M.-C., Decesari, S., Fuzzi, S., Gehrig, R., Hüglin, C., Laj, P., Lorbeer, G., Maenhaut, W., Mihalopoulos, N., Müller, K., Querol, X., Rodriguez, S., Schneider, J., Spindler, G., Brink, H. ten, Tørseth, K., and Wiedensohler, A.: A European aerosol phenomenology – 2: chemical characteristics of particulate matter at kerbside, urban, rural and background sites in Europe, Atmos. Environ., 38, 2579–2595, https://doi.org/10.1016/j.atmosenv.2004.01.041, 2004.

Rinaldi, M., Gilardoni, S., Paglione, M., Sandrini, S., Fuzzi, S., Massoli, P., Bonasoni, P., Cristofanelli, P., Marinoni, A., Poluzzi, V., and Decesari, S.: Organic aerosol evolution and transport observed at Mt. Cimone (2165 m a.s.l.), Italy, during the PEGASOS campaign, Atmos. Chem. Phys., 15, 11327–11340, https://doi.org/10.5194/acp-15-11327-2015, 2015.

Rodríguez González, S., Querol Carceller, X., Universitat Politècnica de Catalunya, and Departament d'Enginyeria Minera i Recursos Naturals: Sources and processes affecting levels and composition of atmospheric particulate matter in the Western Mediterranean, Universitat Politècnica de Catalunya, Barcelona, ISBN 8468809454, 2003.

Salvador, P., Artíñano, B., Viana, M., Alastuey, A., and Querol, X.: Evaluation of the changes in the Madrid metropolitan area influencing air quality: Analysis of 1999–2008 temporal trend of particulate matter, Atmos. Environ., 57, 175–185, https://doi.org/10.1016/j.atmosenv.2012.04.026, 2012.

Samaké, A., Jaffrezo, J.-L., Favez, O., Weber, S., Jacob, V., Albinet, A., Riffault, V., Perdrix, E., Waked, A., Golly, B., Salameh, D., Chevrier, F., Oliveira, D. M., Bonnaire, N., Besombes, J.-L., Martins, J. M. F., Conil, S., Guillaud, G., Mesbah, B., Rocq, B., Robic, P.-Y., Hulin, A., Le Meur, S., Descheemaecker, M., Chretien, E., Marchand, N., and Uzu, G.: Polyols and glucose particulate species as tracers of primary biogenic organic aerosols at 28 French sites, Atmos. Chem. Phys., 19, 3357–3374, https://doi.org/10.5194/acp-19-3357-2019, 2019.

Scerri, M. M., Kandler, K., and Weinbruch, S.: Disentangling the contribution of Saharan dust and marine aerosol to PM_{10} levels

in the Central Mediterranean, Atmos. Environ., 147, 395–408, https://doi.org/10.1016/j.atmosenv.2016.10.028, 2016.

Seabold, S. and Perktold, J.: Statsmodels: Econometric and Statistical Modeling with Python, Python in Science Conference, 28 June–3 July 2010, Austin, Texas, 92–96, https://doi.org/10.25080/Majora-92bf1922-011, 2010.

Seinfeld, J. H. and Pandis, S. N.: Atmospheric chemistry and physics: from air pollution to climate change, 3rd edition., Wiley, Hoboken, New Jersey, 1120 pp., ISBN 9781118947401, 2016.

Spindler, G., Grüner, A., Müller, K., Schlimper, S., and Herrmann, H.: Long-term size-segregated particle (PM_{10}, $PM_{2.5}$, PM1) characterization study at Melpitz – influence of air mass inflow, weather conditions and season, J. Atmos. Chem., 70, 165–195, https://doi.org/10.1007/s10874-013-9263-8, 2013.

Srivastava, D., Tomaz, S., Favez, O., Lanzafame, G. M., Golly, B., Besombes, J.-L., Alleman, L. Y., Jaffrezo, J.-L., Jacob, V., Perraudin, E., Villenave, E., and Albinet, A.: Speciation of organic fraction does matter for source apportionment. Part 1: A one-year campaign in Grenoble (France), Sci. Total Environ., 624, 1598–1611, https://doi.org/10.1016/j.scitotenv.2017.12.135, 2018.

Sun, J., Birmili, W., Hermann, M., Tuch, T., Weinhold, K., Merkel, M., Rasch, F., Müller, T., Schladitz, A., Bastian, S., Löschau, G., Cyrys, J., Gu, J., Flentje, H., Briel, B., Asbach, C., Kaminski, H., Ries, L., Sohmer, R., Gerwig, H., Wirtz, K., Meinhardt, F., Schwerin, A., Bath, O., Ma, N., and Wiedensohler, A.: Decreasing trends of particle number and black carbon mass concentrations at 16 observational sites in Germany from 2009 to 2018, Atmos. Chem. Phys., 20, 7049–7068, https://doi.org/10.5194/acp-20-7049-2020, 2020.

Tomaz, S., Shahpoury, P., Jaffrezo, J.-L., Lammel, G., Perraudin, E., Villenave, E., and Albinet, A.: One-year study of polycyclic aromatic compounds at an urban site in Grenoble (France): Seasonal variations, gas/particle partitioning and cancer risk estimation, Sci. Total Environ., 565, 1071–1083, https://doi.org/10.1016/j.scitotenv.2016.05.137, 2016.

Tomaz, S., Jaffrezo, J.-L., Favez, O., Perraudin, E., Villenave, E., and Albinet, A.: Sources and atmospheric chemistry of oxy- and nitro-PAHs in the ambient air of Grenoble (France), Atmos. Environ., 161, 144–154, https://doi.org/10.1016/j.atmosenv.2017.04.042, 2017.

Valko, M., Morris, H., and Cronin, M.: Metals, Toxicity and Oxidative Stress, Curr. Med. Chem., 12, 1161–1208, https://doi.org/10.2174/0929867053764635, 2005.

Verma, V., Fang, T., Guo, H., King, L., Bates, J. T., Peltier, R. E., Edgerton, E., Russell, A. G., and Weber, R. J.: Reactive oxygen species associated with water-soluble $PM_{2.5}$ in the southeastern United States: spatiotemporal trends and source apportionment, Atmos. Chem. Phys., 14, 12915–12930, https://doi.org/10.5194/acp-14-12915-2014, 2014.

Viana, M., Chi, X., Maenhaut, W., Querol, X., Alastuey, A., Mikuska, P., and Vecera, Z.: Organic and elemental carbon concentrations in carbonaceous aerosols during summer and winter sampling campaigns in Barcelona, Spain, Atmos. Environ., 40, 2180–2193, https://doi.org/10.1016/j.atmosenv.2005.12.001, 2006.

Visentin, M., Pagnoni, A., Sarti, E., and Pietrogrande, M. C.: Urban $PM_{2.5}$ oxidative potential: Importance of chemical species and comparison of two spectrophotometric cell-free assays, Environm. Pollut., 219, 72–79, https://doi.org/10.1016/j.envpol.2016.09.047, 2016.

Waked, A., Favez, O., Alleman, L. Y., Piot, C., Petit, J.-E., Delaunay, T., Verlinden, E., Golly, B., Besombes, J.-L., Jaffrezo, J.-L., and Leoz-Garziandia, E.: Source apportionment of PM_{10} in a north-western Europe regional urban background site (Lens, France) using positive matrix factorization and including primary biogenic emissions, Atmos. Chem. Phys., 14, 3325–3346, https://doi.org/10.5194/acp-14-3325-2014, 2014.

Wang, Y., Wang, M., Li, S., Sun, H., Mu, Z., Zhang, L., Li, Y., and Chen, Q.: Study on the oxidation potential of the water-soluble components of ambient $PM_{2.5}$ over Xi'an, China: Pollution levels, source apportionment and transport pathways, Environ. Int., 136, 105515, https://doi.org/10.1016/j.envint.2020.105515, 2020.

Wappelhorst, S. and Muncrief, R.: How can real-world vehicle emissions data help cities to become zero-emission: some evidence from Europe, TRUE – The Real Urban Emissions Initiative, United Kingdom, https://www.trueinitiative.org/media/749323/true-policy-dialogue-paper-1.pdf (last access: 6 July 2022), 2019.

Weber, S., Uzu, G., Calas, A., Chevrier, F., Besombes, J.-L., Charron, A., Salameh, D., Ježek, I., Močnik, G., and Jaffrezo, J.-L.: An apportionment method for the oxidative potential of atmospheric particulate matter sources: application to a one-year study in Chamonix, France, Atmos. Chem. Phys., 18, 9617–9629, https://doi.org/10.5194/acp-18-9617-2018, 2018.

Weber, S., Salameh, D., Albinet, A., Alleman, L. Y., Waked, A., Besombes, J.-L., Jacob, V., Guillaud, G., Meshbah, B., Rocq, B., Hulin, A., Dominik-Sègue, M., Chrétien, E., Jaffrezo, J.-L., and Favez, O.: Comparison of PM_{10} Sources Profiles at 15 French Sites Using a Harmonized Constrained Positive Matrix Factorization Approach, Atmosphere, 10, 310, https://doi.org/10.3390/atmos10060310, 2019.

Weber, S., Uzu, G., Favez, O., Borlaza, L. J. S., Calas, A., Salameh, D., Chevrier, F., Allard, J., Besombes, J.-L., Albinet, A., Pontet, S., Mesbah, B., Gille, G., Zhang, S., Pallares, C., Leoz-Garziandia, E., and Jaffrezo, J.-L.: Source apportionment of atmospheric PM_{10} oxidative potential: synthesis of 15 year-round urban datasets in France, Atmos. Chem. Phys., 21, 11353–11378, https://doi.org/10.5194/acp-21-11353-2021, 2021.

Xiong, Q., Yu, H., Wang, R., Wei, J., and Verma, V.: Rethinking Dithiothreitol-Based Particulate Matter Oxidative Potential: Measuring Dithiothreitol Consumption versus Reactive Oxygen Species Generation, Environ. Sci. Technol., 51, 6507–6514, https://doi.org/10.1021/acs.est.7b01272, 2017.

Yan, C., Nie, W., Äijälä, M., Rissanen, M. P., Canagaratna, M. R., Massoli, P., Junninen, H., Jokinen, T., Sarnela, N., Häme, S. A. K., Schobesberger, S., Canonaco, F., Yao, L., Prévôt, A. S. H., Petäjä, T., Kulmala, M., Sipilä, M., Worsnop, D. R., and Ehn, M.: Source characterization of highly oxidized multifunctional compounds in a boreal forest environment using positive matrix factorization, Atmos. Chem. Phys., 16, 12715–12731, https://doi.org/10.5194/acp-16-12715-2016, 2016.

Yang, A., Jedynska, A., Hellack, B., Kooter, I., Hoek, G., Brunekreef, B., Kuhlbusch, T. A. J., Cassee, F. R., and Janssen, N. A. H.: Measurement of the oxidative potential of $PM_{2.5}$ and its constituents: The effect of extrac-

tion solvent and filter type, Atmos. Environ., 83, 35–42, https://doi.org/10.1016/j.atmosenv.2013.10.049, 2014.

Yazdani, A., Dillner, A. M., and Takahama, S.: Estimating mean molecular weight, carbon number, and OM / OC with mid-infrared spectroscopy in organic particulate matter samples from a monitoring network, Atmos. Meas. Tech., 14, 4805–4827, https://doi.org/10.5194/amt-14-4805-2021, 2021.

Yu, H., Wei, J., Cheng, Y., Subedi, K., and Verma, V.: Synergistic and Antagonistic Interactions among the Particulate Matter Components in Generating Reactive Oxygen Species Based on the Dithiothreitol Assay, Environ. Sci. Technol., 52, 2261–2270, https://doi.org/10.1021/acs.est.7b04261, 2018.

Zhang, Y., Albinet, A., Petit, J.-E., Jacob, V., Chevrier, F., Gille, G., Pontet, S., Chrétien, E., Dominik-Sègue, M., Levigoureux, G., Močnik, G., Gros, V., Jaffrezo, J.-L., and Favez, O.: Substantial brown carbon emissions from wintertime residential wood burning over France, Sci. Total Environ., 743, 140752, https://doi.org/10.1016/j.scitotenv.2020.140752, 2020.